THESIS FOR THE DEGREE OF DOCTOR OF PHILOSOPHY

Deactivation of after-treatment catalysts for bio-fuelled engines

JOHANNA ENGLUND

CHALMERS

Department of Chemistry and Chemical Engineering
CHALMERS UNIVERSITY OF TECHNOLOGY
Gothenburg, Sweden 2020

Deactivation of after-treatment catalysts for bio-fuelled engines
JOHANNA ENGLUND

ISBN 978-91-7905-282-9

Doktorsavhandlingar vid Chalmers tekniska högskola
Ny serie nr. 4749
ISSN 0346-718X

Department of Chemistry and Chemical Engineering
Chalmers University of Technology
SE-412 96 Gothenburg
Sweden
Telephone +46 (0)31 772 1000

Cover: Illustration of the travel of the molecules from biobased material through fuel and engine exhaust, through the catalytic converter and finally as nitrogen, water and carbon dioxide out from the tailpipe. Made with help from Sigrid and Rut.

Typeset in LaTeX
Printed by Chalmers Reproservice
Gothenburg, Sweden 2020

Deactivation of after-treatment catalysts for bio-fuelled engines

JOHANNA ENGLUND
Department of Chemistry and Chemical Engineering
Chalmers University of Technology

Abstract

To decrease the emissions of anthropogenic CO_2 from vehicles one option is to increase the utilization of biobased fuels. However, there are challenges with this transition, one being the mitigation of emissions of the potent greenhouse gas methane, which is the main constituent of biogas. Another relates to the presence of catalyst poisons in biofuels due to a wide variety of raw materials that are used for the production of these fuels. In this thesis, the aim is to investigate how exhausts from biogas and biodiesel impact the emission control system of a heavy-duty vehicle. The catalysts in the emission control system are studied individually and as a system, with commercial biobased fuels and synthetic gas feeds containing catalyst poisons. After exposure to biogas exhaust for 900 h in an engine-bench, the Pd/Pt-Al_2O_3 oxidation catalyst was found to be severely deactivated in terms of CH_4 oxidation activity. A decrease in low-temperature activity for NO oxidation to NO_2 was observed, which impacts the performance of the SCR-catalyst down-stream in the system. This loss in activity is explained by the finding of catalyst poisons as well as metal segregation and sintering of the noble metal particles. The V_2O_5-WO_3/TiO_2 SCR-catalyst in the engine-bench system remained active for NO_x reduction after long-term ageing, however, the decrease in NO_2 formation over the oxidation catalyst at low temperatures could cause an increase in NO_x emissions even if the SCR catalyst itself is still active. Except for the vanadium-based SCR catalyst also a Cu-CHA catalyst was studied. Both types of SCR catalysts were found to be sensitive to phosphorus poisoning and the Cu-CHA catalyst was also found to be sensitive to sulfur. From results obtained we propose that the SO_2 exposure leads to the formation of Cu-bisulfate species that reduce the amount of copper sites available for NO_x reduction in the Cu-CHA SCR catalyst. The degree of deactivation is also dependent on the reaction condition where the standard SCR reaction is more impacted than the fast SCR reaction.

Keywords: Sustainable transports; Biodiesel; Biogas; Environmental catalysis; Methane oxidation; NO_x reduction; Supported palladium/platinum; Cu-CHA, Vanadium

List of Publications

This thesis is based on the following appended papers:

I. Deactivation of a Pd/Pt bimetallic oxidation catalyst used in a biogas-powered Euro VI heavy-duty engine installation
J. Englund, K. Xie, S. Dahlin, A. Schaefer, D. Jing, S. Shwan, L. Andersson, P.-A. Carlsson, L. J. Pettersson and M. Skoglundh
Catalysts, **9** (2019) 1041.

II. Deactivation of a vanadium-based SCR catalyst used in a biogas-powered Euro VI heavy-duty engine installation
J. Englund, S. Dahlin, A. Schaefer, K. Xie, L. Andersson, S. Shwan, P.-A. Carlsson, L. J. Pettersson and M. Skoglundh
Submitted for publication (2020).

III. Chemical aging of Cu-SSZ-13 SCR catalysts for heavy-duty vehicles -Influence of sulfur dioxide
S. Dahlin, C. Lantto, J. Englund, B. Westerberg, F. Regali, M. Skoglundh and L. J. Pettersson
Catalysis Today, **320** (2019) 72.

IV. Effect of biofuel- and lube oil-originated sulfur and phosphorus on the performance of Cu-SSZ-13 and V_2O_5-WO_3/TiO_2 SCR catalysts
S. Dahlin, J. Englund, H. Malm, M. Feigel, B Westerberg, F. Regali, M. Skoglundh and L. J. Pettersson
Accepted for publication in Catalysis Today (2020).

V. In-situ studies of oxidation/reduction of copper in Cu-CHA SCR-catalysts: Comparison of fresh and SO_2-poisoned catalysts
S.L. Bergman, S. Dahlin, V.V. Mesilov, Y. Xiao, J. Englund, S. Xi, C. Tang, M. Skoglundh, L. J. Pettersson and S.L. Bernasek
Applied Catalysis B: Environmental, 269 (2020) 118722.

My Contributions to the Publications

Paper I

I performed most of the experimental work. I analyzed most of the experimental data and interpreted the results together with my co-authors. I wrote the first draft of the manuscript. I was responsible for writing and submitting the manuscript.

Paper II

I performed most of the experimental work. I analyzed most of the experimental data and interpreted the results together with my co-authors. I wrote the first draft of the manuscript. I was responsible for writing and submitting the manuscript.

Paper III

I performed activity measurements and participated in interpreting data. I co-authored the manuscript.

Paper IV

I participated in the oil-rig ageing experiments and in the interpretation of data. I co-authored of the manuscript.

Paper V

I performed activity measurements and participated in interpreting those data. I co-authored the manuscript.

CONTENTS

CHAPTER 1

INTRODUCTION

The most famous and first definition of Catalysis is the one presented by Jöns Jacob Berzelius in 1835 and he states that catalysis is “the property of exerting on other bodies an action which is very different from chemical affinity. By means of this action, they produce decomposition in bodies, and form new compounds into the composition of which they do not enter" [1]. However, the concept of catalysis was described already in 1794 by Elisabeth Fulhame where she in detail explained how water was needed for combustion of carbon in air [2]. Since the work of both Berzelius and Fulhame was published a lot of progress has been made in the field of catalysis and today it is known that most chemical reactions take place in the presence of catalysts, man-made as well as natural and biological reactions [3–5]. The planet and the humans on it are facing many challenges today in the struggle for survival and unfortunately we, the humans, are causing many of the challenges ourselves. One of the most discussed and critical one is the challenge of climate change which is accelerated by anthropogenic emissions of greenhouse gases and other pollutants from e.g. agriculture, industry and transportation [6].

To deal with emissions from the transportation sector many regulations and legislations have been put in force [7, 8]. In Europe the standards for vehicle emissions are called Euro standards and we are currently enforcing the Euro VI standards [9]. The standard clarifies how much that is allowed to be emitted of a number of pollutants and also for how long these numbers should be obtained. For a heavy-duty truck for instance the defined life time is seven years or 700,000 km whichever occurs first and the allowed

amount of emitted NO_x is 0.4 g/kWh [10, 11].

1.1 Emission control

To be able to comply with emission regulations the vehicle manufacturers have had to implement new technology during the last century [12]. The addition of emission control systems, or exhaust cleaning parts, down-stream of the engine have made a significant difference to the emissions from the transportation sector. These parts are often based on heterogeneous catalysts which means that the catalyst and the reactants/products are in different states, in this case the catalyst is in solid state while the reaction medium is in gas phase [13]. The purpose of the catalyst is to provide an alternative reaction path which is energetically more favourable than the corresponding gas phase reaction while not being consumed itself [14]. The catalyzed reaction is schematically compared to a gas phase reaction in Figure 1.1.

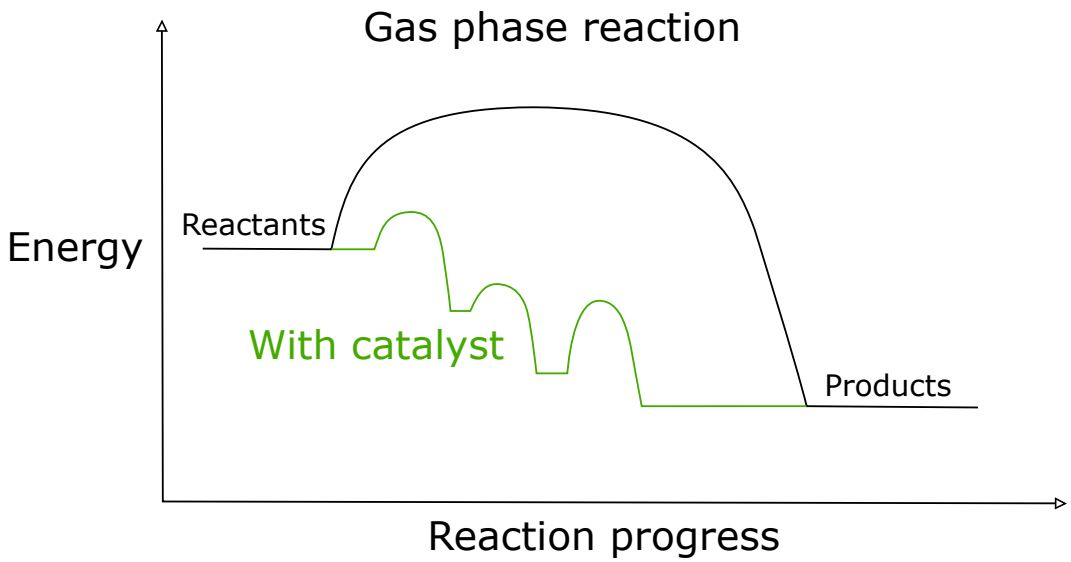

Figure 1.1: An illustration of how a catalyst provides an energetically more favourable reaction path compared to the corresponding gas phase reaction

For petrol powered otto engines the three-way catalyst has been used for emission control since the 1980s [15]. However, the efforts today are focused on reducing CO_2 emissions and thus increase the fuel efficiency. This can be achieved by using an excess of air during the combustion, so-called lean operation. A consequence with lean operation is that the three-way catalyst can not convert the pollutants efficiently since the

operating window in terms of air-to-fuel ratio is narrow around stoichiometric operation. For diesel powered vehicles, and then in particular heavy-duty vehicles, the move towards more lean operation will cause other types of problems since the emission control system is different [16]. Instead of one catalyst that converts carbon monoxide (CO), unburnt hydrocarbons (HC) and nitrogen oxides (NO_x) into less harmful components, like the tree-way catalyst, a modern after-treatment system for a diesel engine powered heavy-duty vehicle application consists commonly of an oxidation catalyst that converts CO and HC into water and carbon dioxide (CO_2) [17], followed by a particulate filter, which collects and converts particulate matter (PM) [18], and an SCR catalyst that reduces the NO_x to nitrogen [19]. The last part in the emission control system is the ammonia slip catalyst (ASC) which oxidizes excess ammonia. For the SCR catalyst to work, a reducing agent needs to be added to the system and the most commonly used one is urea that decomposes and hydrolyzes to ammonia in the exhaust stream above 180 °C [20]. A problem with moving towards more lean operation of the engine is the reduced temperature of the exhaust gases which in turn could mean that the urea, in its current position in the system, would not decompose and hydrolyze into NH_3 and the SCR reaction would halt.

Commonly used oxidation catalysts today are palladium (Pd) and platinum (Pt) supported on alumina (Al_2O_3) [21–26]. The ratio of the metals depends on what type of hydrocarbons that exist in the system. For methane (CH_4), the catalyst tends to have more Pd which is active for CH_4 oxidation, however, some Pt is beneficial for the catalyst system due to stability reasons. The particulate filters used in these systems are usually also catalytic and the catalyst coated on the filter is commonly of similar type as the oxidation catalyst, Pt/Pd on alumina [27, 28]. The state-of-the-art SCR catalyst is metal-exchanged small-pore zeolites and in particular copper-exchanged chabazite (Cu-CHA) [29–35]. The more traditionally used SCR catalyst is the tungsten (W) promoted vanadium (V) catalyst often supported on titania (TiO_2) denoted as V_2O_5-WO_3/TiO_2 [36–42]. There are advantages and disadvantages with all types of catalysts used for emission control today and the aim is always to have a system as active and rigid as possible and the work on improvements of the system is continuously ongoing. When aiming to reduce CO_2 emissions by more fuel-efficient engines that are operating more lean, the general temperature decrease in the exhaust puts a lot of emphasize on the development of catalysts with a good low-temperature activity.

1.2 Biofuels

An additional approach to reduce the amounts of CO_2 emitted from transportation is to move from fossil based fuels towards bio based fuels. The actual amount of CO_2 emitted from the vehicles will not change, however, the carbon in the CO_2 emitted from a bio based fuel will already be part of the carbon cycle as opposed to the carbon from the fossil based fuel. The range of raw materials used for biofuels is wide and many of them are currently not utilized for other products like household waste, which could be used for biogas production [43, 44]. The utilization of bio based raw materials for fuel production is not an end solution since the amount of fuel needed at present is hard to produce without using potential food sources which is not an ethical path to go. Biofuels should be incorporated in our fuels now and the reason is that it is relatively easy and it is much faster than any other solution since the existing infrastructure and vehicle fleet can be used and changes need to happen now. A challenge with introducing new fuels into existing systems is that we do not know how the present aftertreatment is affected. One concern when introducing bio based fuels is that the catalysts will lose activity due to deactivation caused by components in the new fuel, called catalyst poisons.

1.3 Research approach

To study how the introduction of bio based fuels will impact the catalytic emission control system, full scale tests including engine bench testing as well as small lab single poison tests have been utilized in this PhD project. The complexity of the real condition testing is needed due to its similarities with actual conditions and the smaller scales with single poison synthetic exhaust tests provide understanding of how the deactivation occurs. Single components have been studied as well as full systems containing all parts of a full Euro VI engine system. In combination these approaches are powerful in the studies of deactivation of the different catalyst in the emission control system caused by the introduction of biofuels.

1.4 Objectives

The aim of the work presented in this thesis is to study how exhausts from biogas and biodiesel impact the emission control system for heavy-duty vehicles. The impact on individual parts of the emission control system is studied as well as synergy effects through the system. In **Paper I** the impact of biogas exhaust on the performance of a bimetallic Pd-Pt/Al_2O_3 oxidation catalyst is studied. **Paper II** is covering how the V_2O_5-WO_3/TiO_2 SCR catalyst in the same system is impacted by the biogas exhaust. The ageing in the first two papers is conducted in an engine-bench set-up with a full Euro VI emission control system. In **Paper IV** another larger system is used for the ageing, a diesel burner rig. The aim of this paper is to study the impact from two catalyst poisons, phosphorus and sulfur, on both a V_2O_5-WO_3/TiO_2 SCR catalyst as well as a Cu-CHA SCR catalyst when subjected to poison-doped biodiesel. The impact from a up-stream component in the exhaust system is also studied. **Paper III** and **Paper V** are both focusing on single poison, SO_2, deactivation in lab scale and the aim is to evaluate the importance of the SO_2 exposure temperature and to study how the sulfur adsorbs on the active sites of the Cu-CHA SCR catalyst. Additional work is performed on the impact of NO_2 on the degree of deactivation caused by SO_2 exposure.

CHAPTER 2

THE OXIDATION CATALYST

In the engine fuel is ignited in the presence of air. In an ideal case you end up with CO_2 and H_2O since the fuel is a hydrocarbon that burns with oxygen, however, this is not the case in a vehicle engine. In the engine some HC will not be burnt, some of the HC will not be fully oxidized leaving hydrocarbons, partially oxidized hydrocarbons and CO in the exhaust. Furthermore, nitrogen (N_2) and oxygen (O_2) from the air will form NO_x at high temperatures during the combustion process in the engine. Some of the carbon will also form particulate species in a wide size range.

The first component in most Euro VI compliant emission control systems is the oxidation catalyst as shown in Figure 2.1. The main purpose of this catalyst is to oxidize HC and CO into CO_2 and H_2O but, it also oxidizes NO into NO_2 which has consequences for down-stream components such as the particulate filter and the selective catalytic reduction catalyst, which will be discussed later in this thesis.

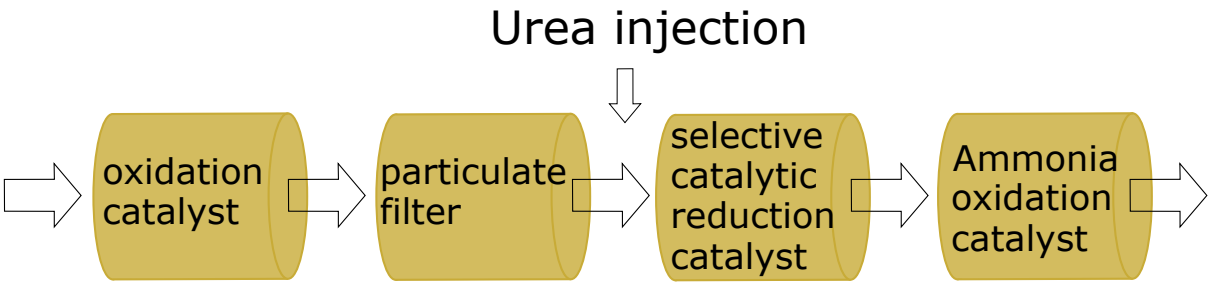

Figure 2.1: Common set-up of the emission control system of a full Euro VI heavy-duty vehicle with oxidation catalyst, particulate filter, selective catalytic reduction catalyst and ammonia oxidation catalyst

2.1 Engine-bench ageing

The oxidation catalyst studied in this thesis has been subjected to biogas exhaust in an engine bench set-up. The engine that has been used is a dual-fuel type engine, which means that 90 % of the fuel was biogas and 10 % was diesel fuel [45, 46]. A more specific and accurate emission control system set-up for the engine-bench ageing, as compared to Figure 2.1, is shown in Figure 2.2. In this case the type of oxidation catalyst is choosen to convert methane efficiently. The particulate filter is commonly called diesel particulate filter since this component is commonly used in vehicles powered by diesel fuel.

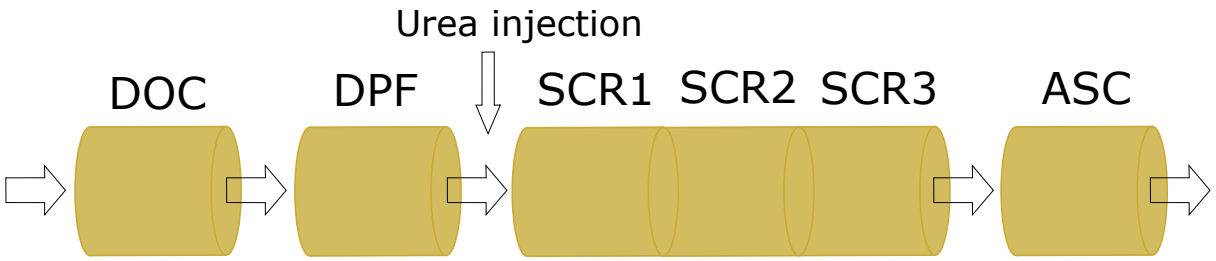

Figure 2.2: Set-up of the emission control system of the Euro VI heavy-duty engine-bench. DOC: oxidation catalyst, DPF: particulate filter, SCR: selective catalytic reduction catalyst, ASC: ammonia oxidation catalyst

The heavy-duty compression ignition engine in the engine-bench set-up was running for 900 h and the mass flow of fuel to the engine was altered to simulate mixed driving. The mass flow was altered to stay withing a temperature range of 170 to 550 °C for the duration of the ageing.

2.2 Catalyst samples

As mentioned in the introduction a commonly used oxidation catalyst is a bi-metallic Pd-Pt catalyst supported on alumina [47–51]. The oxidation catalyst used in this set-up was provided by a catalyst manufacturer. The catalyst was prepared using incipient wetness impregnation which is a commonly used method for preparing this type of catalyst. The Pd:Pt ratio for the catalyst was 2:1 by weight. The reason for choosing this ratio is that the oxidized Pd (PdO) has been found to be active for methane oxidation under lean conditions [52, 53]. Platinum is present in the catalyst as a stabilizer for palladium

which is explained in the introduction. Methane is the main hydrocarbon component in the fuel used in this study. The catalyst is not commercially available and that is due to the high loading of 100 g noble metal/ft^3. The Pd-Pt/Al_2O_3 catalyst was washcoated onto a monolith cordierite substrate with 400 cells per square inch (cpsi) and sample cores with the diameter of 11 mm were drilled out of the main catalyst core and from these sample cores a 19 mm long sample was taken from the inlet part and the outlet part of the engine-bench aged catalyst to be able to detect any axial differences. The engine-bench aged samples were then compared to a fresh catalyst sample.

2.3 Evaluation of catalytic activity in flow reactor

The flow reactor reactor used for evaluation of the catalyst activity before and after exposure to biogas exhaust in the engine-bench consists of a quartz tube heated by a resistive heating coil. The temperature was measured and controlled using thermocouples, one positioned in the center of the catalyst for monitoring the catalyst temperature and the second placed in an un-coated monolith up-stream of the catalyst used for controlling of the catalyst inlet temperature. To maintain an even temperature throughout the reactor the quarts tube was insulated using quartz wool. The gas flow was regulated using mass-flow controllers (MFC) and the water was provided with a controlled evaporator mixer (CEM) system. The reactant flow and the inlet temperature were controlled using a LabVIEW environment [54]. The gas flow used through the reactor tube was 1500 ml/min, which corresponds to a gas hourly space velocity (GHSV) of 45,000 h^{-1}. The effluent gases were analyzed using a Fourier transform infrared (FTIR) spectrometer. Before the activity tests started the sample was subjected to 8 % O_2 in argon at a temperature of 250 °C for a duration of 25 min. The reason for keeping the pre-treatment temperature at such a low temperature was to avoid any regeneration of the samples.

The experimental protocol can be seen in Table 2.1. The results from performing the experiments according to this protocol are presented in **Paper I** and the main figure is re-printed in Figure 2.3. In window a) and d) the conversion of methane is shown for the fresh oxidation catalyst (DOC ref), and the inlet (DOC in) and outlet (DOC out) parts of the engine bench aged oxidation catalyst as a function of temperature for two different gas feeds. The top row results are collected in a complex gas feed consisting

of all three reactants, CO, NO and CH_4, while the results shown in the bottom row is collected from experiments with only one of these reactants.

Table 2.1: Experimental protocol for oxidation activity tests. Base feed for all experiments: 8 vol.-% O_2, 5 vol-% H_2O and Ar used as balance. The temperature was increased and decreased linearly by 5 °C/min.

Temperature [°C]	CO [vol.-ppm]	CH_4 [vol.-ppm]	NO [vol.-ppm]	Description
100-450↑↓	1000	-	-	CO oxidation
100-450↑↓	-	1000	-	CH_4 oxidation
100-450↑↓	-	-	1000	NO oxidation
100-450↑↓	1000	1000	1000	Complex mixture of gases

From the methane oxidation experiments in Figure 2.3a) and d) it is clearly shown that the samples that have been exposed to biogas exhaust for 900 h have lost considerably in activity for CH_4 oxidation. It is also evident that the presence of the other reactants, NO and CO, is beneficial for the CH_4 oxidation reaction. During oxidation of hydrocarbons like methane, hydroxyl (OH) groups are formed on the surface of the catalyst and it is believed that NO will remove some of these groups leaving more active sites available for CH_4 to adsorb and be oxidized [55]. From the results for CH_4 oxidation it is also evident that the inlet sample is slightly more deactivated than the outlet sample of the oxidation catalyst. The reason for this is discussed in section 2.4.

An additional observation that can be made in Figure 2.3 is that the NO oxidation conversion profiles, Figure 2.3b) and e), are quite different for the samples exposed to biogas exhaust in the engine-bench compared to the profiles for the fresh oxidation catalyst. At lower temperatures less NO is oxidized to NO_2 while at higher temperatures exposure to biogas exhaust appears to be beneficial for the NO_2 formation. The oxidation of NO to NO_2 plays an important role for the regeneration of the particulate filter and for the NO_x reduction in the SCR catalyst placed down-stream in the system. The peak of the NO conversion profile also splits into two peaks for the engine-bench aged samples, which is an indication of Pd-Pt segregation and sintering since large Pt particles are particularly active for NO oxidation [56]. The existence of mono-metallic and larger particles are also shown in section 2.4.

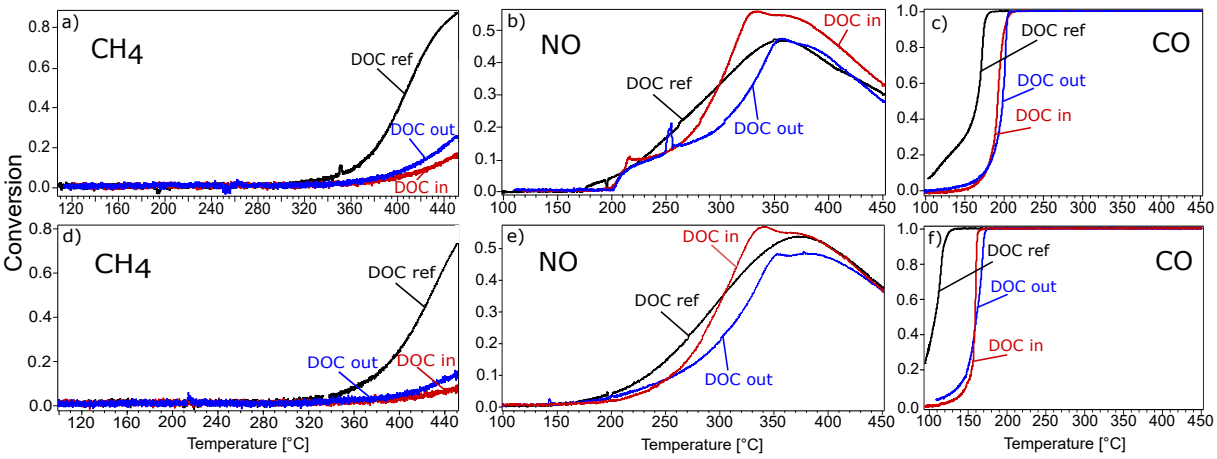

Figure 2.3: Conversion during heating of a) and d) CH_4, b) and e) NO and c) and f) CO over the fresh Pd-Pt/Al_2O_3 oxidation catalyst (DOC ref), and the inlet (DOC in) and outlet (DOC out) of the engine bench aged Pd-Pt/Al_2O_3 oxidation catalyst. Top row, a-c, in a feed consisting of 1000 ppm CH_4, 1000 ppm NO, 1000 ppm CO, 8 % H_2O, 5 % O_2, and Argon as balance. Bottom row, d-f, in a feed consisting of 1000 ppm CH_4 or 1000 ppm NO or 1000 ppm CO with 8 % H_2O, 5 % O_2, and Argon as balance.

2.4 Catalyst characterization

Performing activity measurements of the catalyst samples is a good way to measure deactivation since the performance of the sample is shown. However, to be able to improve the catalyst system or to understand differences caused by the engine-bench ageing, the catalyst samples need to be characterized. There are several characteristics of the catalyst that could be impacted by exposure to biogas exhaust. The most important are the size and surface composition of the noble metal particles providing the active sites and the presence of catalyst poisons on the surface of the catalyst. By using different characterization techniques it is possible to determine how these traits are impacted which is crucial to provide understanding about the deactivation mechanisms.

Surface composition

In heterogeneous catalysis the chemical reactions take place on the surface of the catalyst which means that determining the physical structure and chemical composition of the surface is crucial. There are many techniques that could be used to elucidate the physical structure and chemical composition of a catalyst and they all come with advantages and disadvantages which means that it could be beneficial to use more than one technique depending on what characteristic that is of interest. The following techniques

have been used to quantify which catalyst poisons that are deposited on the surface after exposure to biogas exhaust in an engine-bench for 900 h, where on the catalyst they are found and in what chemical state they are found.

XRF

X-ray fluorescence (XRF) is a quantitative measurement technique, which works well when comparing the concentration of elements in samples. However, the exact number might not be completely accurate. The measurement is made on a pellet which contains the catalyst sample ground into a powder mixed with a binder. The sample is irradiated with X-rays of high energy. The irradiation ejects electrons from the inner orbitals causing electron holes. These holes are filled by electrons from higher orbitals and when they jump down in energy, fluorescent radiation is emitted and the energy of this radiation is characteristic for each element, just like a fingerprint. The fingerprint can then be compared to references with known concentrations of each element and that is how you determine and quantify the elements present in the sample [57].
When performing XRF measurements on the inlet and outlet sample of the engine-bench aged Pd-Pt/Al_2O_3 oxidation catalyst and compare it to the reference sample in **Paper I** it was found that sulfur and phosphorus were the main components in the group of catalyst poisons. Sulfur was found on both the inlet and outlet samples at a concentration level of around 0.25 wt.% while the concentration of phosphorus was about 0.2 wt.% on the inlet sample and 0.04 wt.% on the outlet sample.

SEM-EDX

From the XRF analysis we know that sulfur is present in equal concentrations on both the inlet and outlet samples of the engine-bench aged Pd-Pt/Al_2O_3 catalyst and that phosphorus is mainly found on the inlet sample. Using scanning electron microscopy (SEM) with an energy-dispersive X-ray analysis system it is possible to distinguish where in the washcoat the elements are more concentrated. In **Paper I** the SEM-EDX measurement was performed on the cross-cut of a small piece of the monolith sample. The sample is subjected to an electron beam which excites electrons to a higher energy level leaving a hole behind. When this hole is filled by an electron from a higher energy level, X-rays of certain unique energies for each element, are emitted and detected.

In Figure 2.4 it is clear that phosphorus is found in higher concentrations on the surface of the washcoat of the inlet sample while sulfur is more evenly distributed over the catalyst and throughout the washcoat.

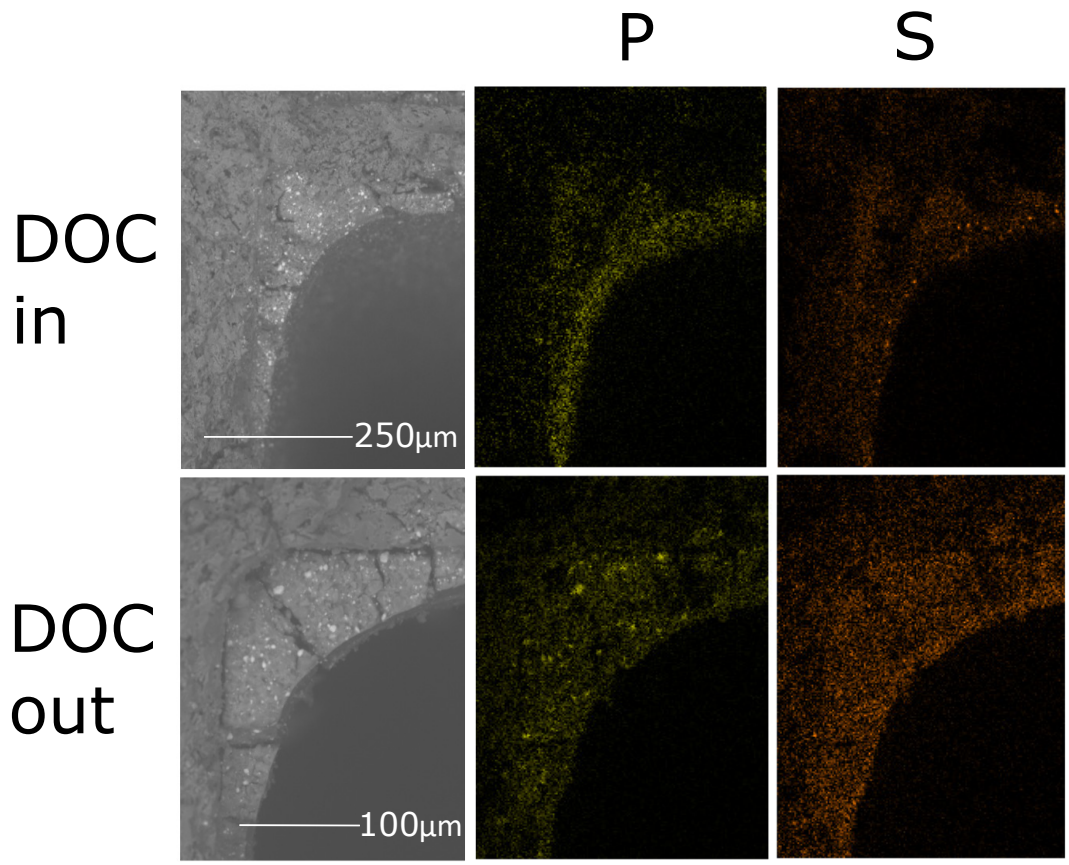

Figure 2.4: SEM images and EDX maps of P and S for the inlet (DOC in) and outlet (DOC out) parts of the engine bench aged Pd-Pt/Al_2O_3 oxidation catalyst (**Paper I**).

XPS

Using X-ray photoelectron spectroscopy (XPS) it is possible to determine in which chemical state the elements are present on the surface of the sample [58]. In **Paper I** a small piece of a monolith wall is subjected to an X-ray beam while the number of electrons that leave the surface and the kinetic energy of those electrons is measured. This gives information about the element and its chemical surrounding. Since the SEM-EDX analysis showed that phosphorus mainly is present on the surface of the washcoat of the inlet sample we wanted to investigate if the chemical state of phosphorus present here is different from the state of phosphorus on the outlet of the engine-bench aged sample.

As can be seen in Figure 2.5 phosphorus in the form of P_2O_5 is only found in the inlet sample. This compound is known as phosphate glass and it sticks to the first surface it comes in contact with. Furthermore phosphate glass is hard to remove which means that the deactivation caused by this compound is irreversible.

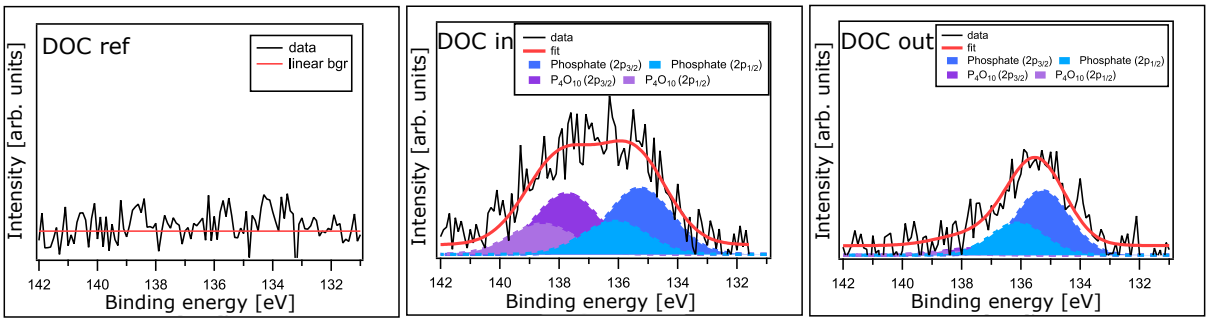

Figure 2.5: Phosphorus 2p core level spectra for the fresh Pd-Pt/Al_2O_3 oxidation catalyst (DOC ref) and of the inlet (DOC in) and outlet (DOC out) parts of the engine bench aged Pd-Pt/Al_2O_3 oxidation catalyst (**Paper I**)

Particle size and composition

Using X-ray techniques gave insight about which elements and the chemical state of those elements that where present on the catalyst and where those elements and compounds are found. As mentioned previously more characteristics of the catalyst are of importance and from the activity measurements indications of metal segregation and sintering were observed.

NO oxidation

From the NO oxidation experiments in **Paper I** it was observed that the oxidation catalyst, after engine-bench ageing, had developed a double peak for the NO conversion profile as can be seen in Figure 2.6. The catalyst used is a bi-metallic Pd-Pt/Al_2O_3 catalyst and in terms of NO oxidation platinum shows high activity and then in particular larger Pt particles [56]. The split of the NO conversion profile into two peaks indicates that there are two different types of sites where NO oxidation takes place, one being more efficient at lower temperatures which is consistent with the presence of larger Pt particles indicating sintering and segregation of the active Pd and Pt metals.

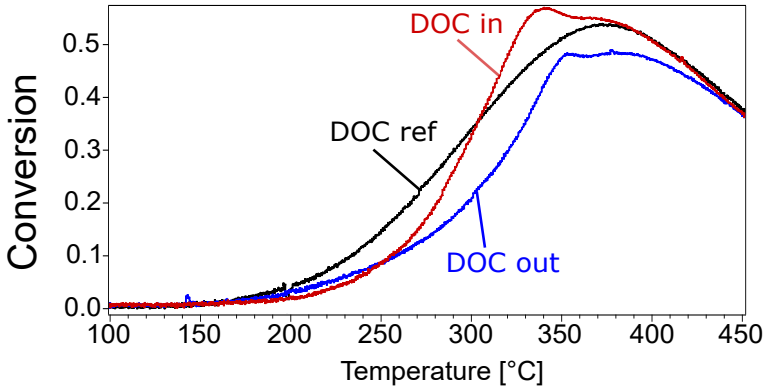

Figure 2.6: Conversion of NO during heating for the fresh Pd-Pt/Al_2O_3 oxidation catalyst (DOC ref), and the inlet (DOC in) and outlet (DOC out) of the engine bench aged Pd-Pt/Al_2O_3 oxidation catalyst. Feed gas composition during the experiment: 1000 ppm NO, 8 % O_2 and 5 % H_2O with argon as balance (**Paper I**).

TEM

Using transmission electron microscopy (TEM) in scanning mode (STEM) with a high angle annular dark field (HAADF) detector makes it possible to observe the metal particles on the catalyst as white dots. From the images shown in Figure 2.7 it is possible to measure the size of the noble metal particles in the Pd-Pt/Al_2O_3 catalyst studied in **Paper I**. However, the particles are too small to distinguish between palladium and platinum in the instrument used. The size of 100 particles was measured for each sample and the average particle size increased from 4.0 nm for the fresh sample to 9.5 nm for the inlet sample and 8.0 nm for the outlet sample of the engine-bench aged catalyst. Not only the average particle size increased, also the maximum particle size increased from 9.0 nm to 20 nm for the engine-bench aged samples.

XRD

From the TEM analysis it is clear that the particle size increases after exposure to biogas exhaust and using X-ray diffraction it is also possible to observe that mono-metallic particles appear after the exposure. To perform the XRD measurements in **Paper I** washcoat of the Pd-Pt/Al_2O_3 catalyst was scraped off from the monolith samples and spread over a silicon wafer. The sample was irradiated with monochromatic X-rays while changing the incident angle between 30 and 90 °. The obtained diffraction pattern is unique for each crystalline component. By using this technique it was shown that, after

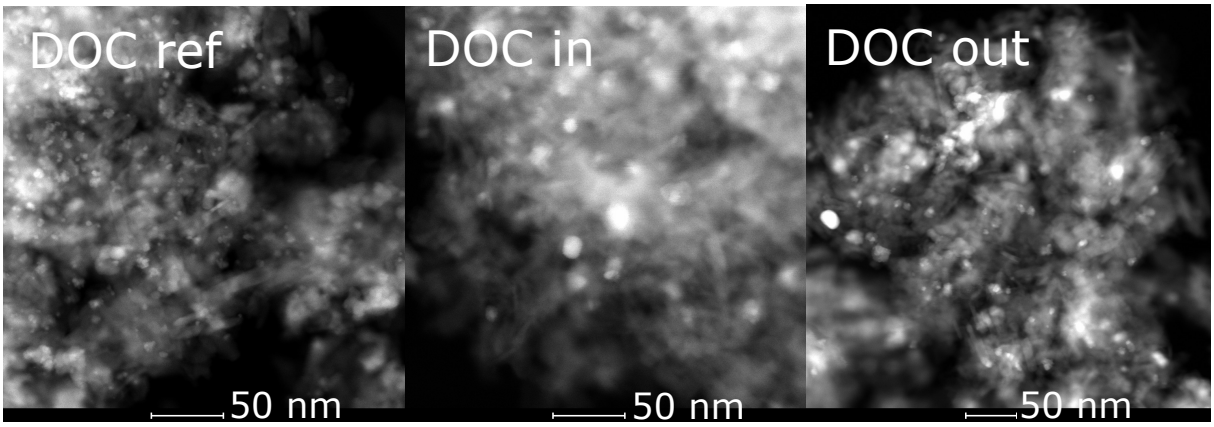

Figure 2.7: TEM images of the fresh Pd-Pt/Al_2O_3 oxidation catalyst (DOC ref) and the inlet (DOC in) and outlet (DOC out) of the engine bench aged Pd-Pt/Al_2O_3 oxidation catalyst (**Paper I**).

exposure to biogas exhaust, mono-metallic particles (crystals) of Pd and Pt are present in those samples.

Active sites

When the elements on the the catalyst surface is known, as well as the state of the noble metal particles in terms of size and Pd-Pt segregation, it is interesting to connect this to the number of active sites on the catalyst. To quantify the number of active sites in **Paper I**, CO chemisorption was used. In the CO chemisorption analysis 3x3 channels were cut out from each sample and confined between folded quartz wool in a quarts U-tube. To have reliable and reproducible results the samples were oxidized for 1 h at 350 °C followed by evacuation and then reduction for 1 h. During cooling to 35 °C, which was the temperature used for CO chemisorption, the sample was evacuated and the evacuation continued for 10 min when the desired temperature was reached. CO was dosed until a pressure of 600 mmHg was reached. The amount of CO adsorbed at this point is assumed to be both chemisorbed and physisorbed, and by performing the measurement a second time the physisorbed amount is obtained. By subtracting the adsorbed amount of CO from the two measurements the amount of CO that is chemisorbed on the catalyst sample was obtained. The amount of chemisorbed CO for each mol of Pd/Pt decreased from 0.06 to 0.001 for the inlet sample and to 0.003 for the outlet sample which is a significant decrease. From the TEM analysis it was found that the Pd-Pt particles sintered into larger particles after engine-bench ageing and this causes the number of active surface sites to decrease which is part of the explanation

to the decreased amount of adsorbed CO on the samples taken from the engine-bench aged Pd-Pt/Al_2O_3 oxidation catalyst. An other part of the explanation is the presence of catalyst poisons on the engine-bench aged catalyst samples, which block surface Pd-Pt atoms causing a decrease in the number of active surface sites where CO could adsorb.

2.5 Summary of the results for the oxidation catalyst

By subjecting a full emission control system to exhaust from a dual-fuel engine powered by biogas and a small portion of diesel for ignition for 900 h, the deactivation of the first component, the oxidation catalyst, is found to be severe in terms of activity for methane oxidation. Not only the methane oxidation reaction is impacted, the CO oxidation is shifted towards higher temperatures which mean that at low loads, CO will not efficiently be converted into CO_2. The oxidation of NO into NO_2 is also impacted from exposure to biogas exhaust. At lower temperatures less NO is converted into NO_2 when compared to a fresh oxidation catalyst and at higher temperatures the opposite is the case especially for the inlet sample of the aged catalyst which showed a higher conversion of NO to NO_2. The decrease in NO_2 formation at lower temperatures will impact the performance of the down-stream SCR catalyst which benefits from the presence of NO_2 in the exhaust stream. The reason for the loss in activity towards methane oxidation and the shift in light-off for the CO oxidation is caused by the presence of catalyst poisons like sulfur and phosphorus on the engine-bench aged samples partially covering the active Pd and Pt sites, and by sintering and segregation of the Pd/Pt particles into larger mono-metallic particles which results in fewer available surface Pd and Pt sites. Following the oxidation catalyst in the emission control system is the particulate filter and also this part is impacted from the loss in NO_2 formation at lower temperatures since NO_2 promotes the regeneration process of the filter. To investigate how the particulate filter is impacted from exposure to biogas exhaust, the following chapter will deal with that specific component of the emission control system.

CHAPTER 3

THE PARTICULATE FILTER

Many emission control set-ups, especially in heavy-duty vehicles, have a particulate filter which purpose is to reduce particulate matter emissions form the vehicle [27,28,59–61]. Particulte filters could be both catalytic and non-catalytic. The purpose of making the filter catalytic is to oxidize NO into NO_2, which is a more efficient oxidizing agent than O_2 in terms of oxidizing carbonaceous species. This type of regeneration of the particulate filter, where the temperature is not increased, is called passive regeneration and the presence of a catalyst improves this reaction [62]. The passive regeneration is improved by the up-stream oxidation catalyst which also provides NO_2 for oxidation of carbonaceous particulate matter. The emissions of PM have decreased since legislations and standards were introduced, however the size of the PM has also decreased over time and the new nano-sized PM is significantly more toxic and dangerous to human health then the larger sized PM present when the engines were less efficient [61].

3.1 Filter samples

The work performed on particulate filters in this thesis is limited to the engine-bench ageing study with a full Euro VI emission control system connected to a dual-fuel heavy-duty engine powered by biogas and a small portion of diesel for 900 h. The particulate filter used in this set-up was coated with a Pt/Al_2O_3 catalyst. Some Pd was also found on the outlet part of the filter which could be part of the washcoated catalyst or it could have been deposited there after desorption from the oxidation catalyst. Every other

channel of the filter is plugged in the outlet which means that there will be an accumulation of poisons on the outlet part of the filter in contrary to the oxidation catalyst. The elemental composition of the inlet and outlet part of the filter was analyzed after 900 h exposure to biogas exhaust.

3.2 Elemental analysis

The elemental composition of the aged particulate filter we evaluated using XRF. The method and procedure is described in section 2.4.

XRF

The results from the XRF measurements in **Paper II** are shown in table 3.1. As is evident from these results some of the phosphorus that passed through the oxidation catalyst ended up in the particulate filter as well as the known catalyst poisons sulfur, calcium and zink. As was shown for the oxidation catalyst, the presence of catalyst poisons impacts the oxidation of NO into NO_2 and at lower temperatures the NO_2 formation decreases after exposure to biogas exhaust in the engine-bench. Since the type of catalyst coated on the filter is of similar type as the Pd-Pt/Al_2O_3 oxidation catalyst, the same phenomenon is likely applicable for this part of the emission control system as well. This will cause a decrease of passive regeneration which means that the need for active regeneration of the particulate filter will increase.

Table 3.1: Content of P, S, Ca and Zn in the inlet and outlet parts of the particulate filter (DPF in and DPF out resp.) as obtained by XRF analysis. *The binder used when preparing the samples contains 82 ppm phosphorus.

Sample	Phosphorus [ppm]	Sulfur [ppm]	Calcium [ppm]	Zink [ppm]
DPF in	600*	890	380	160
DPF out	900*	1300	1000	480

As was shown for the oxidation catalyst, the presence of catalyst poisons impacts the oxidation of NO into NO_2 and at lower temperatures the NO_2 formation decreases after exposure to biogas exhaust in the engine-bench. Since the type of catalyst coated on the filter is of similar type as the oxidation catalyst, the same phenomenon is likely applicable for this part of the emission control system as well. This will cause a decrease of passive regeneration by NO_2 which means that active regeneration of the particulate filter will need to be applied more often. Active regeneration is performed by burning fuel more rich to increase the temperature and this leads to an increased fuel consumption, so-called fuel penalty, which impacts the overall fuel-efficiency of the vehicle [63].

CHAPTER 4

THE SCR CATALYST

With the oxidation catalyst HC, CO and some of the NO are oxidized forming water, CO_2 and NO_2. NO_2 assists in the passive regeneration of the particulate filter, which is the next part of the emission control system, while the other two reaction products are of no benefit for the reactions in the emission control system. The components upstream of the SCR catalyst in the emission control system are not only producing NO_2, which is beneficial for regeneration of the particulate filter as well as for the reduction of NO_x in the SCR catalyst, but they play another important as well as undesired role, they collect catalyst poisons. This is of course detrimental to their own performance but it also hinders the poisons to reach the SCR catalyst, which can retain its performance for a longer duration of time. From the results for the oxidation catalyst it is clear that the different catalyst poisons interact differently with the catalyst. Phosphorus mainly adsorbs on the first surface it comes in contact with, which means that it will take longer time for this poison to reach the SCR catalyst in a Euro VI compliant system, like the one presented in Figure 2.1. Sulfur on the other hand is transported through the system and reaches the SCR catalyst faster than phosphorus. How resistant the SCR catalyst is towards catalyst poisons depends on which type of SCR catalyst that is used. The traditionally used catalyst is a vanadium based catalyst promoted by tungsten and supported on titania. The state-of-the-art catalyst though is the copper-exchanged chabazite (Cu-CHA) catalyst. As mentioned in the introduction these catalysts both have advantages and disadvantages. The sulfur tolerance of the vanadium based catalyst is an important advantage, however the need for active regeneration of the particulate

filter can lead to temperature spikes that may cause thermal degradation of the catalyst [64,65] while the copper-exchanged zeolite can withstand higher temperatures without losing activity [66–68]. The Cu-CHA catalyst is however sensitive to sulfur poisoning which is why sulfur poisoning of this type of catalysts is an important research topic [69–71]. The SCR studies presented in this thesis have been performed in scales ranging from single poison in lab scale to full vehicle driving on the road.

4.1 Engine-bench ageing

The results for the oxidation catalyst and the particulate filter from ageing in the engine-bench have been presented in chapter 2 and 3, respectively, and the scheme and set-up for the ageing experiment have been described in section 2.1. In Figure 4.1 the SCR part of the emission control system used in the engine-bench ageing is presented and as can be seen three consecutive SCR catalysts were used in this set-up.

Figure 4.1: Set-up of the SCR part of the emission control system of an Euro VI compliant heavy-duty vehicle. DPF: particulate filter, SCR: selective catalytic reduction catalyst, ASC: ammonia oxidation catalyst

Catalyst samples

The SCR catalyst used in the engine-bench set-up in **Paper II** is a V_2O_5-WO_3 type catalyst impregnated on a fiberglass-reinforced TiO_2 in a corrugated shape. Samples were taken from the inlet and the outlet parts of the first and last SCR catalyst and they were designated according to Table 4.1. The reason for taking samples from the inlet and outlet parts of the first and last SCR catalyst was to investigate whether or not any axial differences throughout the SCR catalysts could be observed.

Table 4.1: Description of the engine-bench aged V_2O_5-WO_3/TiO_2 SCR catalyst samples.

Sample name	Description
SCR-fresh	Fresh sample of the SCR catalyst
SCR1-in	Inlet sample of the first engine-bench aged SCR catalyst
SCR1-out	Outlet sample of the first engine-bench aged SCR catalyst
SCR3-in	Inlet sample of the third and last engine-bench aged SCR catalyst
SCR3-out	Outlet sample of the third and last engine-bench aged SCR catalyst

Evaluation of catalytic activity in flow reactor

The catalyst performance was evaluated in terms of SCR performance which means how well it converts NO_x from the exhaust stream to N_2 with NH_3 as reducing agent. There are three main reaction routes for NO_x removal, standard, fast and NO_2 rich SCR. Which route the reaction follows depends on the ratio between NO_2 and NO in the exhaust stream.

Standard SCR

When only NO is present as NO_x source, the reaction route that is followed is called standard SCR and the overall reaction can be seen schematically in equation 4.1 [72–75]. Depending on the type of catalyst used and the sites available on the catalyst, the actual reaction path for NO_x reduction on the catalyst may differ [76, 77]. For vanadium based catalysts the reaction proceeds via a redox cycle, where vanadium alters between V^{5+} and V^{4+}. Ammonia adsorbs on V=O (V^{5+}) sites, which in presence of NO are reduced to V-OH (V^{4+}) sites, whereby N_2 and H_2O are formed. The V-OH sites are finally reoxidized to V=O sites by O_2 and the cycle is closed [76, 78]. For Cu-CHA catalysts, the reaction also proceeds via a redox cycle, where copper alters between Cu^{2+} and Cu^{+}. The adsorbed NH_3 and NO react on Cu^{2+} sites forming N_2 and H_2O whereby the Cu^{2+} sites are reduced to Cu^{+} sites. The Cu^{+} sites are finally reoxidized to Cu^{2+} by O_2, closing the redox cycle [77, 79].

$$4\ \mathrm{NO} + 4\ \mathrm{NH_3} + \mathrm{O_2} \rightarrow 4\ \mathrm{N_2} + 6\ \mathrm{H_2O} \tag{4.1}$$

Fast SCR

When the concentration of NO_2 in the exhaust stream increases due to the existence of an oxidation catalyst up-stream in the system, the reaction follows the path called fast SCR. The overall reaction of this path is shown in equation 4.2.

$$2\ NO + 4\ NH_3 + 2\ NO_2 \rightarrow 4\ N_2 + 6\ H_2O \tag{4.2}$$

The presence of NO_2 facilitates the reoxidation of V^{4+} to V^{5+} and Cu^{+} to Cu^{2+}, which is considered as the rate-limiting step for the SCR reaction at low temperatures [76, 79]. The third route where there is a stoichiometric excess of NO_2 is sometimes referred to as slow SCR and this reaction path should be avoided [80].

In **Paper II** the NO_x reduction performance for the V_2O_5-WO_3/TiO_2 catalyst was analyzed before and after exposure to biogas exhaust for 900 h. The results for all three SCR conditions show similar trends but different absolute numbers. The NO_x conversion decreases only slightly for the catalyst samples exposed to biogas exhaust as compared to the fresh catalyst as is evident by Figure 4.3 and 4.2. Below 300 °C there is a slight loss in activity towards NO_x reduction under fast and standard SCR conditions for the samples exposed to biogas exhaust in the engine-bench and then mainly for the samples taken from the first SCR catalyst.

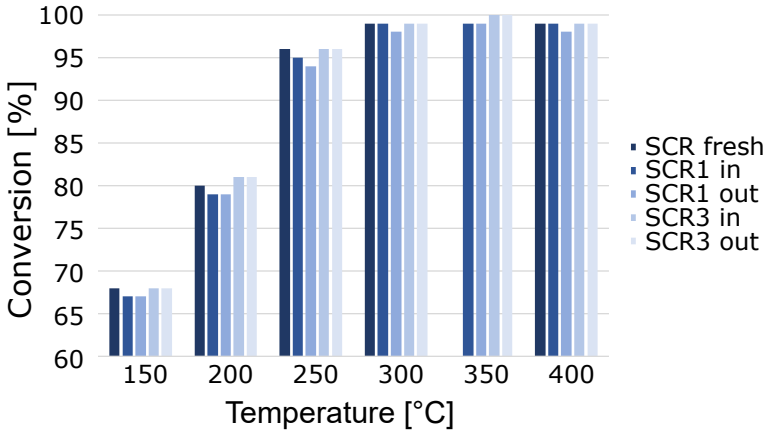

Figure 4.2: Conversion of NO_x over the fresh V_2O_5-WO_3/TiO_2 SCR catalyst (SCR-fresh), the inlet and outlet samples of SCR catalyst 1 (SCR1-in and SCR1-out resp.) and the inlet and outlet samples of SCR catalyst 3 (SCR3-in and SCR3-out resp.) at steady state for six temperatures, 150, 200, 250, 300, 350 and 400 °C at standard SCR conditions. The feed consisted of 1100 ppm NH_3, 1000 ppm NO, 8 % O_2, 5 % H_2O and argon as balance. Note the cut off y-axis (**Paper II**).

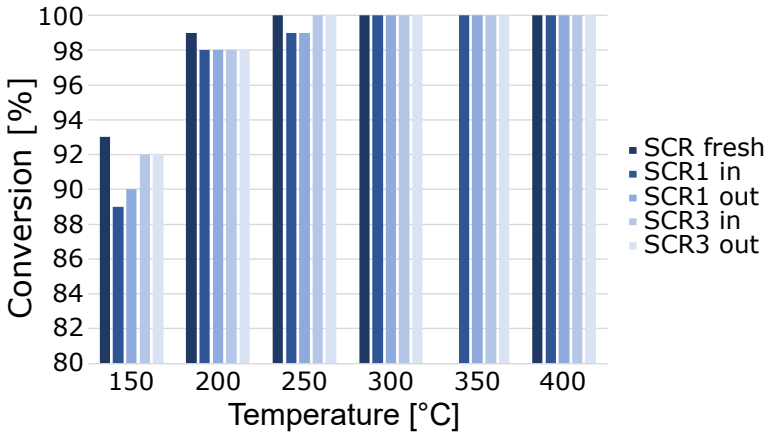

Figure 4.3: Conversion of NO_x over the fresh V_2O_5-WO_3/TiO_2 SCR catalyst (SCR-fresh), the inlet and outlet samples of SCR catalyst 1 (SCR1-in and SCR1-out resp.) and the inlet and outlet samples of SCR catalyst 3 (SCR3-in and SCR3-out resp.) at steady state for six temperatures, 150, 200, 250, 300, 350 and 400 °C at fast SCR conditions. The feed consisted of 1100 ppm NH_3, 500 ppm NO, 500 ppm NO_2, 8 % O_2, 5 % H_2O and argon as balance. Note the cut off y-axis (**Paper II**).

Catalyst characterization

Even if the deactivation of the V_2O_5-WO_3/TiO_2 SCR catalysts, in terms of NO_x conversion, appears to be low after biogas exhaust exposure, the catalyst samples were characterized and analyzed to be able to detect other potential changes to the catalyst. We know from the results of the oxidation catalyst in chapter 2 and the particulate filter in chapter 3 that an accumulation of known catalyst poisons was found in these parts of the emission control system. It was also found that phosphorus appears to adsorb mainly on the inlet of the emission control system, while other poisons like sulfur are dispersed more evenly over the emission control system.

Elemental analysis and surface composition

By using XRF in **Paper II** a small amount of sulfur was found in the engine-bench aged samples. However no sulfur or phosphorus of significant amounts were found in the samples using XPS. The presence of sulfur detected by XRF is mainly found on the outlet samples of the SCR catalysts as seen in Table 4.2. However, when using XPS no significant signal in the S 2p region could be detected for the engine-bench aged samples as can be seen from the survey spectra in Figure 4.4. The reason for these conflicting results could be that XPS is a highly surface sensitive characterization technique [81],

and the amount of sulfur falls below the detection level, while XRF probes the bulk composition of the whole sample. No phosphorus of significant amount was found using XRF and even if a low signal for phosphorus is observed in the P 2p region using XPS, see Figure 4.4, the intensity of the P 2p signal is constant for all samples and does not change after exposure to biogas exhaust.

Table 4.2: Content of catalyst poisons in the V_2O_5-WO_3/TiO_2 SCR catalyst samples measured by XRF.

Sample	Phosphorus [%]	Sulfur [ppm]	Calcium [ppm]	Zink [ppm]
SCR-fresh	0.19*	400	1.7	-
SCR1-in	0.17*	630	1.5	-
SCR1-out	0.20*	820	1.6	-
SCR3-in	0.18*	650	1.5	-
SCR3-out	0.18*	840	1.6	-

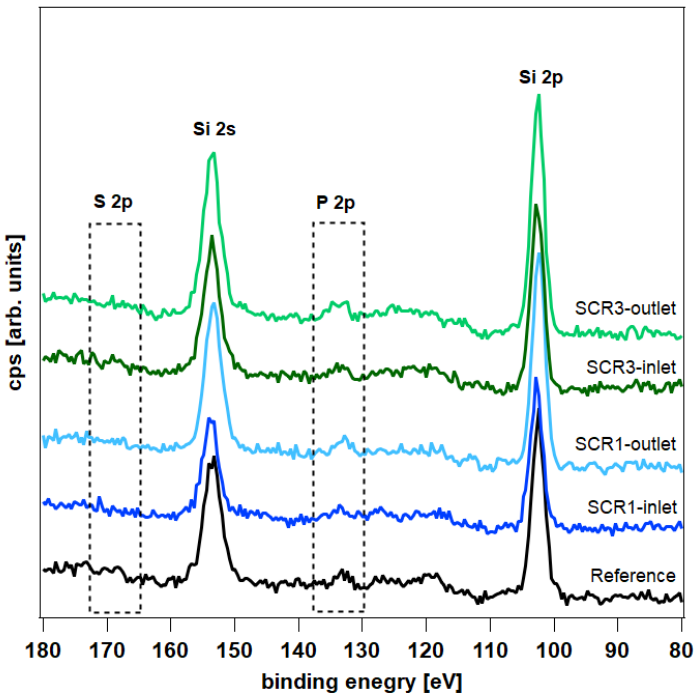

Figure 4.4: XPS survey spectra of the fresh V_2O_5-WO_3/TiO_2 SCR catalyst (SCR-fresh), the inlet and outlet samples of SCR catalyst 1 (SCR1-in and SCR1-out resp.), the inlet and outlet samples of SCR catalyst 3 (SCR3-in and SCR3-out resp.). The S 2p and P 2p regions are marked with boxes (**Paper II**).

Not only the catalyst poisons are of interest when characterizing the elements on the catalyst, the nature of the active species is also relevant to study. When studying how the vanadium species on the V_2O_5-WO_3/TiO_2 catalyst change after exposure to biogas exhaust for 900 h XPS is useful since different oxidation states of the element can be distinguished as is evident in Figure 4.5. Especially the inlet sample from the first SCR catalyst shows a significant shift in the V^{5+} (V_2O_5) to V^{4+} (VO_2) ratio which indicates that the vanadium sites partially are blocked and not reoxidized to V^{5+}.

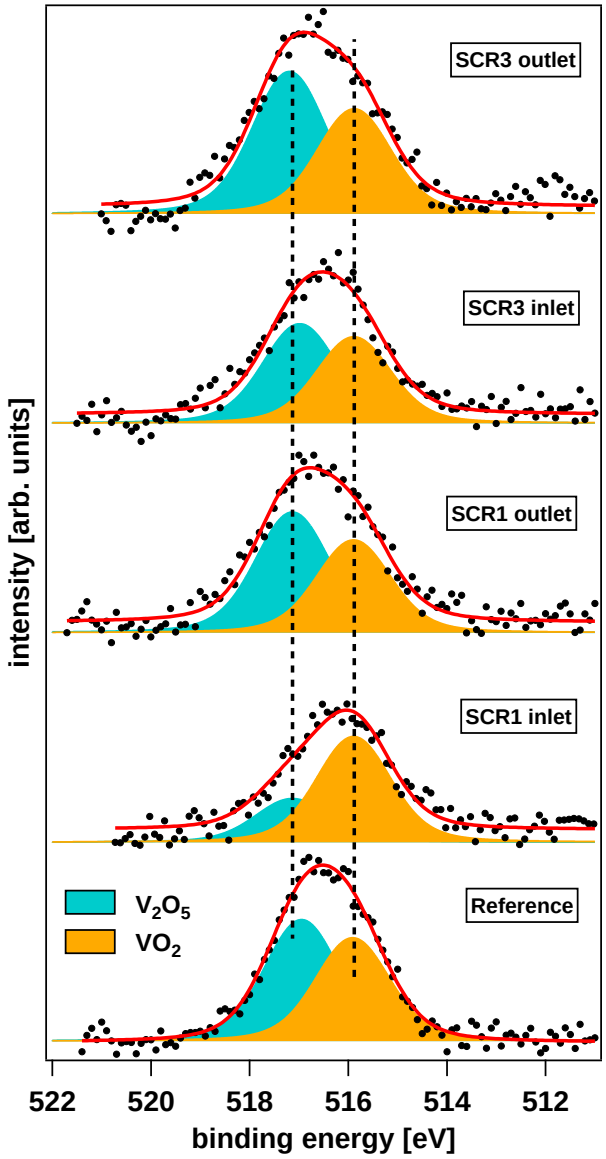

Figure 4.5: Vanadium $2p_{3/2}$ core level spectra of the fresh V_2O_5-WO_3/TiO_2 SCR-catalyst (Reference) and the inlet and outlet samples of SCR catalyst 1 and 3, respectively (**Paper II**).

NH_3-TPD

The acidity of the V_2O_5-WO_3/TiO_2 SCR catalyst before and after exposure to biogas exhaust in **Paper II** was characterized using NH_3-TPD. The results are summarised in Table 4.3 and shows decreased amounts of desorbd ammonia from the engine-bench aged samples, especially the outlet parts of the SCR catalysts. The TPD experiment was performed by subjecting the samples to NH_3 in argon for the duration of 1 h at a temperature of 150 °C. The system was then flushed with argon and then subjected to a heating ramp with a rate of 10 °C/min up to 400 °C in an atmosphere consisting of water and argon whereby the amount of desorbed NH_3 was detected.

Table 4.3: Desorption of NH_3 during a heating ramp relative to the desorption for the SCR-fresh sample. Temperature for maximum NH_3 desorption, T_{max}, is also presented. The feed during the heating ramp consisted of 5 % H_2O in argon. GHSV: 45,000 h^{-1}.

Sample	Desorbed amount of NH_3 [% of SCR-fresh]	T_{max} [°C]
SCR-fresh	100	236
SCR1-in	76	253
SCR1-out	48	229
SCR3-in	87	238
SCR3-out	48	226

4.1.1 Summary of the ageing results for the engine bench aged SCR-catalyst

The SCR catalyst is located as the third component in the emission control system used in the engine-bench ageing and due to this it appears that most of the catalyst poisons present in the exhaust feed will not reach this component. Some sulfur was found on the analyzed samples but the performance of the SCR catalysts was only slightly affected. A low decrease in activity towards NO_x reduction was observed at lower temperatures for the inlet part of the engine-bench aged sample. This could be due to hindering of the reoxidation of V^{4+} to V^{5+}, essential in the catalytic cycle, which is indicated by the XPS results in Figure 4.5. Over a temperature of 300 °C no significant decrease in activity

for NO_x reduction is observed for the engine-bench aged samples. However, even if only a minor deactivation in terms om NO_x reduction performance was observed, other changes to the catalyst were seen. The outlet samples of both the first and last SCR catalyst showed a considerably reduced ability to adsorb NH_3 which is linked to the higher concentrations of sulfur in these samples blocking the acidic sites for ammonia adsorption. As mentioned previously, the first part of the SCR catalyst (SCR1-in) showed a considerably higher ratio of V^{4+} to V^{5+} compared to the fresh sample which indicates that the redox cycle for parts of the active sites is blocked which in turn results in reduced NO_x reduction performance.

4.2 Diesel burner ageing

Another way of simulating real ageing of an emission control system is by using a diesel burner set-up. In **Paper IV** the set-up consists of a fuel feed, air feed and a diesel burner, and can be seen in Figure 4.6. The samples were placed in a sample holder displayed in Figure 4.6b) and there where four SCR catalysts used in each aging experiment, two Cu-CHA samples and two V_2O_5-WO_3/TiO_2 samples. Up-stream of one of each of the SCR catalysts, a dummy (an un-coated cordierite substrate) was mounted and in front of the other an oxidation catalyst was mounted. Five of the channels had only dummies in them.

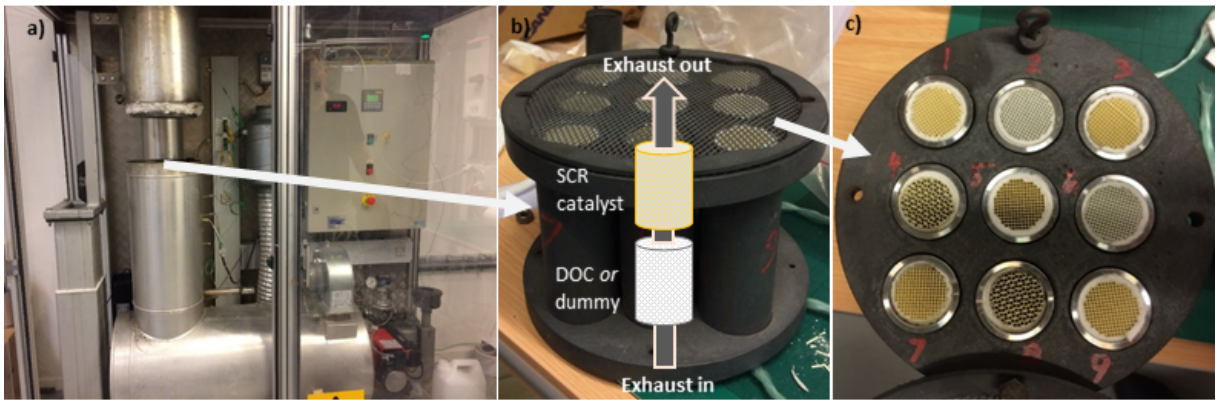

Figure 4.6: The diesel burner aging rig (a) and sample holder (b and c). For each aging, the sample holder was loaded with four SCR catalyst cores, two DOC cores (in front of two of the SCR catalysts) and the remaining channels (1, 3, 5, 7, 9) were filled with dummies (**Paper IV**).

The fuel used in this study was a biodiesel of FAME (fatty acid methyl ester) type and the aim of this particular study was to study how the exposure to exhaust from biodiesel doped with known amounts of catalyst poisons impacts the two types of SCR catalysts used. The aim was also to investigate if the impact on the SCR catalysts was different if a dummy or an oxidation catalyst was placed up-stream. The catalyst poisons used were phosphorus, in the form of triphenyl phosphate (TPP), and sulfur, in the form of dipropyl disulfide (DPDS). The aim was to subject the catalysts to a lifetime of phosphorus and sulfur exposure. To calculate what amount of TPP and DPDS that corresponds to a lifetime exposure, assumptions were made. The amount of P and S in a standard biodiesel was assumed to be 4 and 5 ppm, respectively, and the fuel consumption was estimated to 30 kg/100 km and the catalyst real weight to be 5 kg. Based on these

assumptions and a known concentration of phosphorus and sulfur in TPP and DPDS, these compounds were added to the biodiesel barrels. One experiment was performed with only phosphorus added and one with only sulfur. The third poisoned barrel contained a mixture of both phosphorus and sulfur but the concentrations of each poison in this barrel corresponded to 10 % of a lifetime exposure. The obtained concentrations of catalyst poisons can be seen for each barrel, including the reference without added poisons, in Figure 4.7. The ageing lasted for roughly 150 h and the temperature was around 450 °C for the duration of the ageing. The combustion of the fuels was performed with an excess of oxygen in the feed to the burner.

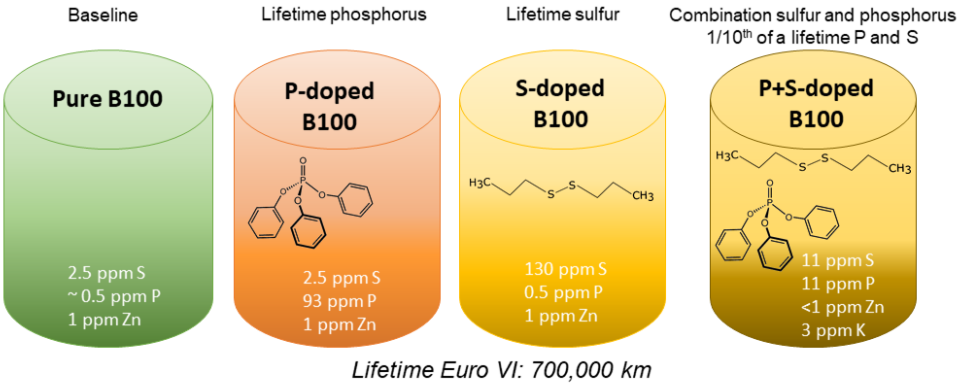

Figure 4.7: The fuels used in the four experiments, B100 is pure biodiesel of FAME type. Figure reprinted with permission from S. Dahlin [82].

Catalyst samples

The two SCR catalysts used in this study are the most common catalysts used for heavy-duty vehicle SCR. The vanadium based one is the same catalyst used in the engine-bench study with biogas as fuel which means it is a V_2O_5-WO_3 type catalyst impregnated on a fiberglass-reinforced TiO_2 in a corrugated shape. The second SCR catalyst is the one that is used in the rest of the SCR studies in this thesis, a copper-exchanged CHA catalyst washcoated on a cordierite substrate. Details about the catalysts can be seen in **Paper IV**. The oxidation catalyst that was placed up-stream of one each of the SCR catalyst was a bi-metallic Pt-Pd/Al_2O_3 catalyst with a 2:1 ratio in terms of weight and a loading which was 20 g noble metal/ft^3 . This catalyst is different when compared to the catalyst used in chapter 2 and that is because this one is optimized for biodiesel exhaust while the other one used was optimized for biogas exhaust.

SCR performance

The NO_x reduction performance was measured under standard SCR condition in a gas bench flow reactor which is described in **Paper III** and **Paper V**. Before the samples were aged they where evaluated using the same protocol as after the diesel burner ageing and the details can be seen in Table 4.4 and **Paper IV**.

Table 4.4: Activity test procedure. GHSV: 120,000 h^{-1} with 10 % O_2 and 5 % H_2O in N_2. The procedure was performed at both 220 and 280°C.

Step	NO (vol.-ppm)	NO_2 (vol.-ppm)	NH_3 (vol.-ppm)	Description
1	1000	0	0	Ref. NO_x concentration standard SCR
2	500	500	0	Ref. NO_x concentration fast SCR
3	250	750	0	Ref. NO_x concentration NO_2-rich SCR
4	0	0	0	N_2
5	0	0	1000	Saturation with NH_3 and ref. NH_3 conc.
6	1000	0	1000	Standard SCR activity
7	250	750	1000	NO_2-rich SCR activity
8	500	500	1000	Fast SCR activity
9	1000	0	0	Removal of NH_3 from the surface and ref. NO concentration

The catalyst performance was measured at six isotherms between 200 and 500 °C. After exposure to exhaust from the diesel burner for 150 h the V_2O_5-WO_3/TiO_2 catalyst does not show and significant change in SCR performance when exposed to pure biodiesel or sulfur-doped biodiesel when compared to the fresh catalyst, see Figure 4.8. The catalyst exposed to sulfur-doped fuel even show a slight improvement in SCR performance when compared to the fresh sample when an oxidation catalyst (DOC) is placed in front of the SCR catalyst. However, when a dummy is placed up-stream of the vanadium based SCR catalyst, deactivation in terms of NO reduction performance, is seen from 300 °C even for the sample exposed to exhaust from sulfur-doped fuel. When phosphorus is present as dopant in the fuel, the deactivation is much more severe especially for the SCR catalyst with a dummy up-stream. The deactivation is especially seen at lower and intermediate temperatures, at the maximum test temperature most of the activity

is restored for all samples when compared to the fresh sample. The combination of phosphorus and sulfur as dopant appears to have a considerable detrimental effect on the NO_x reduction performance for the V_2O_5-WO_3/TiO_2 catalyst in absence of an oxidation catalyst present up-stream. From the results shown in Figure 4.8 it is clear that phosphorus is a strong catalyst poison for this type of SCR catalyst while sulfur is not. The latter is in line with previous studies, the vanadium based SCR catalyst is robust against sulfur poisoning [83, 84].

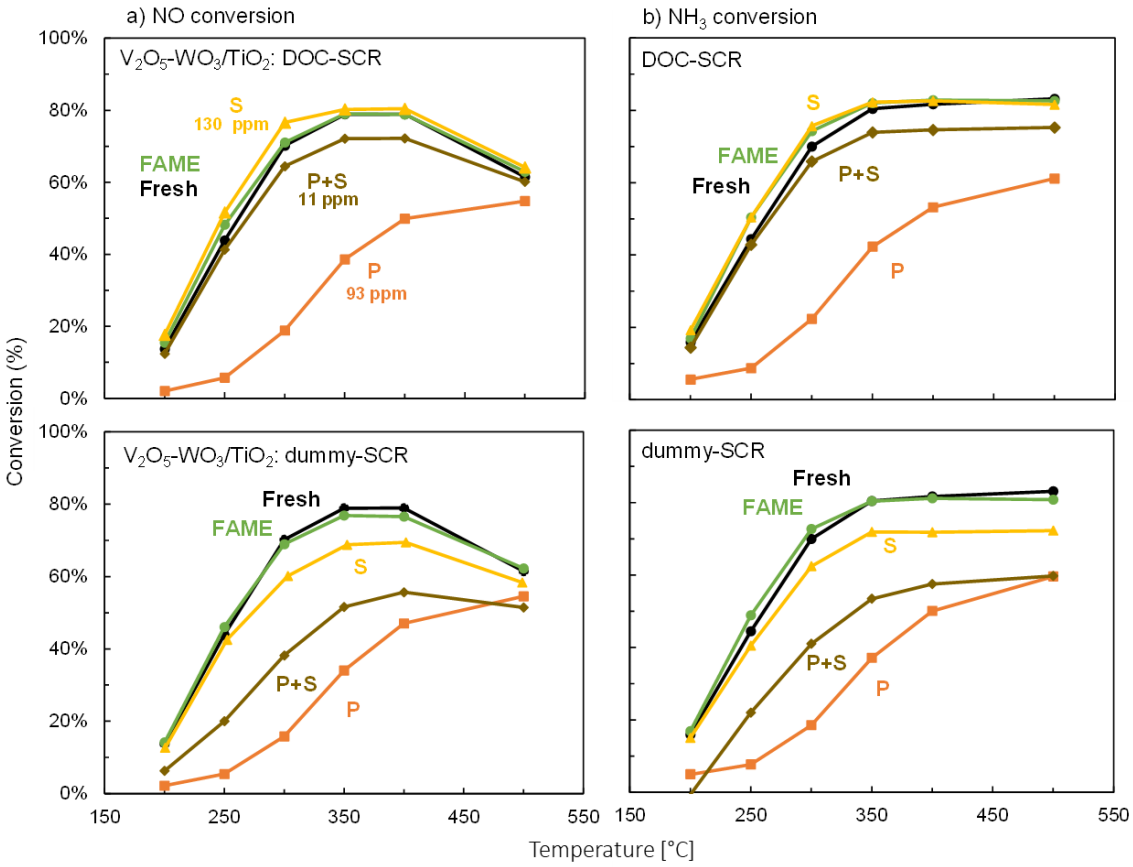

Figure 4.8: Effect of exposure to pure (green), P- (orange), S- (yellow), and S+P-doped (brown) biodiesel (FAME) exhaust on NO and NH_3 conversion of the V_2O_5-WO_3/TiO_2 catalyst. DOC-SCR (top row) or dummy-SCR (bottom row) configuration during aging. Test conditions: 10 % O_2, 1000 ppm NO and NH_3, 5 % H_2O, GHSV 120,000 h^{-1} (**Paper IV**).

When comparing the results for the V_2O_5-WO_3/TiO_2 catalyst in Figure 4.8 with the corresponding results for the Cu-SSZ-13 catalyst in Figure 4.9, it is clear that the performance of the fresh SCR catalyst, especially at lower temperatures, is significantly better for the Cu-SSZ-13 catalyst. However when exposed to sulfur-doped fuel the per-

formance of the Cu-SSZ-13 catalyst at low and intermediate temperatures decreases severely. The same trend as for the V_2O_5-WO_3/TiO_2 catalyst is seen for the Cu-SSZ-13 catalyst where an up-stream placed Pt-Pd/Al_2O_3 oxidation catalyst results in less severe deactivation of the SCR catalyst. When the fuel is doped with phosphorus almost no NO_x conversion is observed until 350 °C where some conversion is seen. For the Cu-CHA catalyst, which does not possess the same sulfur resistance as the vanadium based catalyst, the exhaust from the sulfur-doped fuel is detrimental to the NO conversion and the impact appears to be similar even in the presence of an up-stream Pt-Pd/Al_2O_3 catalyst. When both dopants were present (S+P), the effect of the up-stream DOC appears to be more significant than for the other experiments and this was also seen when the samples were characterized.

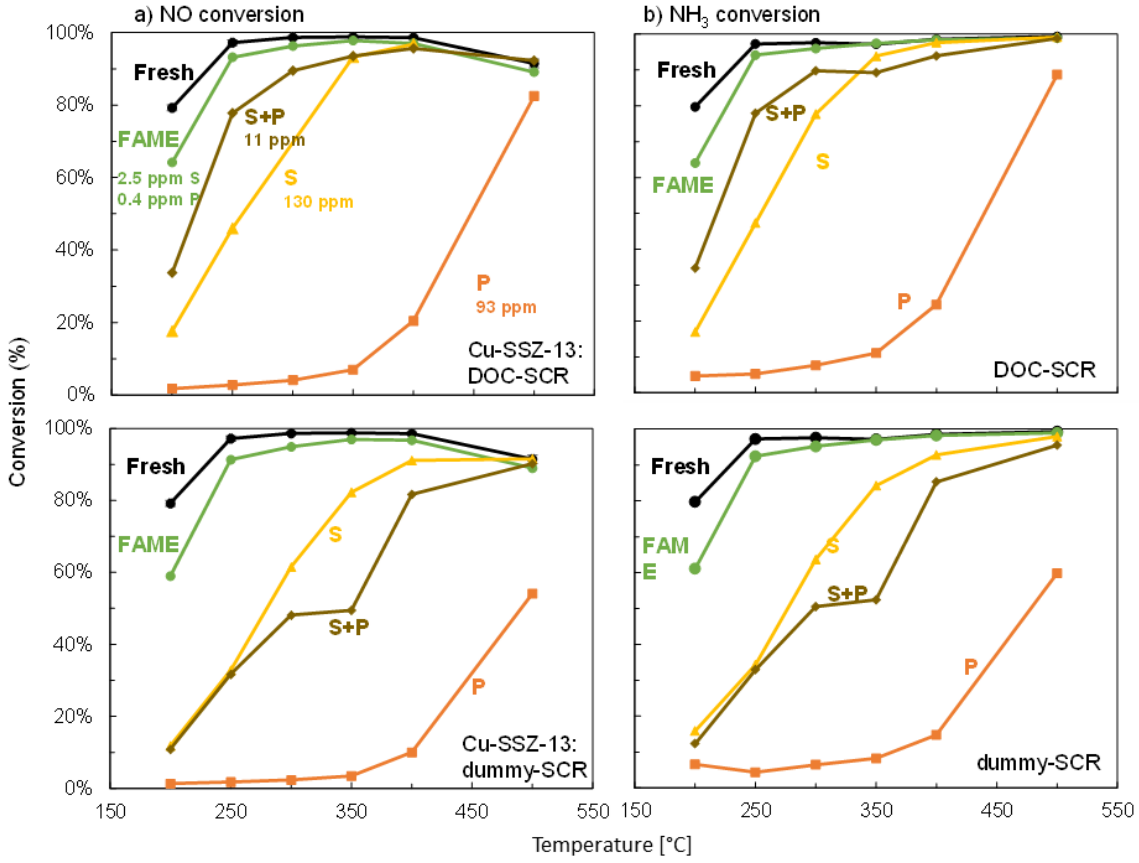

Figure 4.9: Effect of exposure to pure (green), P- (orange), S- (yellow), and S+P-doped (brown) biodiesel (FAME) exhaust on NO and NH_3 conversion of he Cu-CHA catalyst. DOC-SCR (top row) or dummy-SCR (bottom row) configuration during aging. Test conditions: 10 % O_2, 1000 ppm NO and NH_3, 5 % H_2O, GHSV 120,000 h^{-1} (**Paper IV**).

Catalyst characterization

To determine where and how much of the doped poisons that was adsorbed on the catalysts after exposure to exhaust from the diesel burner, a Leco sulfur analyzer was used for sulfur. It combust the sample in oxygen and the formed SO_2 is then detected using a non-dispersive infrared (NDIR) sensor. For the quantification of phosphorus and other elements, XRF was used. For the oxidation catalyst discussed in chapter 2, it was clear that phosphorus mainly adsorbs on the inlet part of the catalyst. However, for the SCR catalyst exposed to exhausts from phosphorus-doped fuel in this study the same concentration of phosphorus was found throughout both types of SCR catalysts. The ratio of phosphorus to vanadium in the vanadium based catalyst was high which means that a considerable amount of the phosphorus in the exhaust was captured by this catalyst. The measured amount of phosphorus by XRF was around 2 wt% which resulted in a P/V ratio of almost 3. This means that phosphorus does not only adsorb on the vanadium sites in this catalyst but also on other sites. For the Cu-CHA catalyst, the measured P/Cu ratio was close to 1 when a dummy was placed up-stream and closer to 0.8 in presence of a Pt-Pd/Al_2O_3 catalyst. The higher amount of phosphorus adsorbed on the sample with a dummy placed up-stream is likely the explanation to why this sample shows a higher degree of deactivation when compared to the sample with a Pt-Pd/Al_2O_3 catalyst placed up-stream. The phosphorus to active metal ratio indicates that phosphorus adsorbs more selectively to the copper sites on the Cu-CHA catalyst when compared to the vanadium sites on the V_2O_5-WO_3/TiO_2 catalyst. When decreasing the phosphorus concentration in the fuel and adding sulfur the presence of a Pt-Pd/Al_2O_3 catalyst up-stream of the SCR catalyst a considerable impact on the NO_x reduction was observed which can be seen in Figure 4.8 and 4.9. The same is seen when the elemental composition was measured, when a Pt-Pd/Al_2O_3 oxidation catalyst was placed up-stream the SCR catalyst, the P/V ratio was close to zero while it was 1.2 with a DOC present up-stream of the V_2O_5-WO_3/TiO_2 SCR catalyst. For the Cu-CHA catalyst, the P/Cu ratio was 0.49 with a dummy present and $<$0.24 with a DOC present up-stream of the SCR catalyst. For these experiments with lower concentration of dopant in the fuel, an axial effect was also seen over both types of SCR catalysts where a higher concentration of phosphorus was found in the inlet part of the samples than in the outlet part which is in agreement with what was found for the oxidation

catalyst in chapter 2.

4.2.1 Summary of the ageing results for the oil rig aged SCR-catalyst

After exposure to exhaust from biodiesel doped with sulfur or phosphorus, or the combination of both, the NO_x reduction performance under standard SCR conditions changes for both the Cu-CHA catalyst as well as the V_2O_5-WO_3/TiO_2 SCR catalyst. The copper-exchanged catalyst is sensitive to both poisons, however phosphorus was shown to be a strong catalyst poison for this type of catalyst. The same is seen for the vanadium based catalyst, however, this catalyst actually gained some activity after exposure to sulfur-doped biodiesel exhaust. The two types of catalysts seem to adsorb phosphorus differently where Cu-CHA adsorbs the phosphorus selectively on the active metal sites while the V_2O_5-WO_3/TiO_2 catalyst also adsorbs phosphorus on other sites than the vanadium sites.

The presence of an oxidation catalyst up-stream of the SCR catalyst has many implications on the performance of the SCR catalyst, independently of the type of SCR catalyst. One beneficial aspect of the oxidation catalyst on the direct performance of the SCR catalyst is the formation of NO_2, which is beneficial for the NO_x reduction performance of the SCR catalyst. Another more long term effect which was found from the diesel burner ageing experiments is that the oxidation catalyst appears to be a buffer for the SCR catalyst, by adsorbing catalyst poisons which delays the deactivation of the SCR catalyst. However, the deactivation of the oxidation catalyst, caused by accumulation of catalyst poisons, could in turn lead to lower formation of NO_2, which is negative for the overall performance of the SCR catalyst.

4.3 Single poison ageing

Up until this part of the thesis the ageing of the catalysts has been performed in engine-bench and diesel burner scale. From now on the scale will be smaller and the catalyst poison used will be sulfur. The focus from here on will also be on one specific SCR catalyst, the state-of-the-art Cu-CHA catalyst and its low-temperature SCR activity. For the understanding of how the deactivation of the catalyst takes place during poisoning the small scale, single poison ageing is necessary. The poison used in this section is SO_2 which is known to be a detrimental catalyst poison for the Cu-CHA catalyst, which was also shown in section 4.2 where the presence of sulfur in the fuel resulted in a considerable degradation of the catalyst in terms of NO_x reduction performance. Several aspects of the SO_2 exposure have been studied, the significance of the SO_2 exposure temperature, which type of copper sites that are impacted by SO_2 exposure and the effect of SCR conditions i.e. with no, 50 % and 75 % NO_2 as NO_x source in the feed.

Catalyst samples

The samples used for the single poison ageing were the same type of samples that were used throughout, a copper-exchanged chabazite zeolite, Cu-CHA, with a copper loading of 2.5 % and a Si/Al ratio of around 15. This is the same sample which is investigated in **Paper III, IV** and **V**. The catalyst was washcoated onto a cordierite monolith substrate and in the case where powder sample is needed, washcoat was scraped off from the monolith substrate.

Poison exposure

The samples in this section have all been subjected to sulfur in the same form and with the same procedure. The form of sulfur used for the ageing was SO_2, which is a common state for sulfur in the exhaust from a heavy-duty engine [85]. The ageing with SO_2 was performed in gas flow reactors with 50 ppm SO_2 present in the feed together with 5 % H_2O and 10 % O_2 using N_2 or argon as balance. The exposure temperature ranged between 210 and 400 °C and the space velocity was kept constant at 45,000 or 60,000 h^{-1}.

One of the aims with the single poison ageing experiments was to investigate the impact

of the SO_2 exposure temperature on the degree of deactivation, as mentioned previously, which is why that temperature ranged from 210 to 400 °C.

SCR performance

To evaluate the catalysts performance before and after exposure to SO_2, SCR experiments using standard, fast and NO_2 rich conditions were performed. For determining at which temperature the SO_2 exposure is most detrimental to the SCR catalyst, SCR experiments under standard, fast and NO_2 rich conditions were performed at 220 and 280 °C. After activity test the catalyst was exposed to SO_2 at a temperature between 220 and 400 °C and then the activity was measured under standard SCR conditions once again. The sulfur exposed samples are named SX where the X represents the exposure temperature. In Figure 4.10 the relative rate constant can be seen for samples exposed to SO_2 at different temperatures. The rate constant is calculated based on the NO_x conversion and then related to the rate constant of the fresh sample to achieve the relative rate constant. The details about the calculations can be found in equation 4.3. From Figure 4.10 it is evident that the lower the SO_2 exposure temperature the lower the relative rate constant. This means that the catalysts performance in terms of NO_x reduction which is most severely affected by SO_2 exposure at low temperatures. The low temperature for SO_2 exposure is thus the temperature used for further studies.

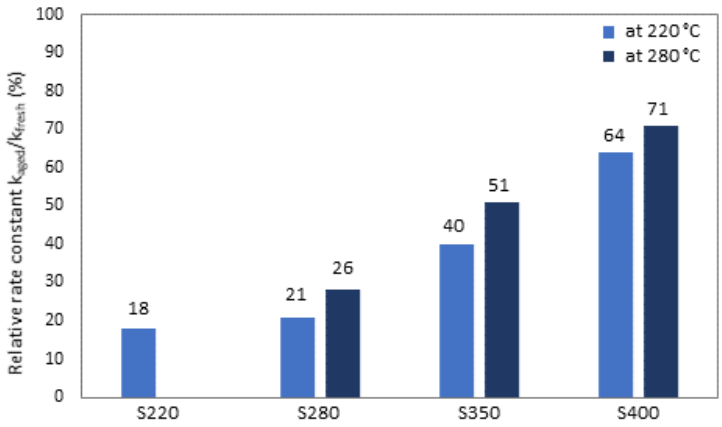

Figure 4.10: Relative rate constants at 220 and 280 °C respectively during standard SCR conditions for Cu-CHA catalysts exposed to SO_2 220, 280, 350 and 400 °C. Note, the sample exposed to SO_2 at 220 °C was not tested at 280 °C. 1000 ppm NO, 1000 ppm NH_3, 10 % O_2, 5 % H_2O, GHSV of 120,000 h^{-1} during the activity test (**Paper III**).

To elucidate what actually happens with the catalyst after SO_2 exposure, the Cu-CHA catalyst was tested at different SCR conditions to investigate if the different SCR cycles are impacted differently by the SO_2 exposure. It is clear from the results presented in Figure 4.11 that the presence of NO_2 in the gas feed is beneficial for the NO_x reduction performance of the catalyst after SO_2 exposure. After regeneration in water and oxygen at 500 °C (R500) and at 700 °C (R700) for 30 min, most or all of the activity could be regained which indicates that the sulfur does not adsorb permanently on the active sites of the catalyst. The same trend where the NO_x conversion decreases significantly more under standard SCR conditions compared to fast SCR conditions is shown in **Paper III**. In **Paper III** as well as **Paper V**, the ability to regain most of the activity after regeneration at elevated temperatures is proven which corresponds well with previous studies [86–95].

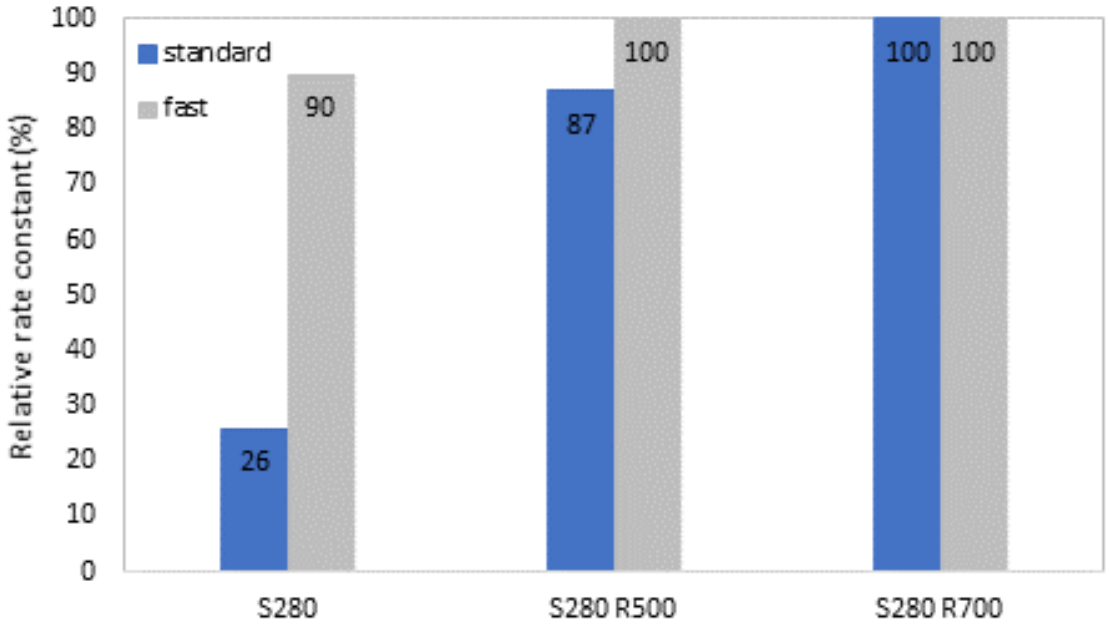

Figure 4.11: Relative rate constants at 280 °C, for the Cu-CHA catalyst exposed to SO_2 at 280 °C. 1000 ppm NO_x (NO_2/NO_x = 0, and 0.5 respectively) 1000 ppm NH_3, 10 % O_2, 5 % H_2O, GHSV of 120,000 h^{-1} during the activity test (**Paper III**).

The importance of the presence of NO_2 during NO_x reduction can also be seen in Table 4.5 where the NO_x conversion decreased significantly after SO_2 exposure under standard SCR conditions. For the samples used to collect the data in Table 4.5 only minor

deactivation was observed under fast SCR conditions which implies that the oxidation of NO into NO_2 under standard SCR conditions is hindered after SO_2 exposure.

Table 4.5: NO_x conversion for a fresh and SO_2-exposed Cu-CHA SCR catalyst. NO_x conversion after regeneration at 500 and 700 °C is also presented. The SO_2 exposure was performed at 220 °C. The gas feed composition for each of the SCR experiments, standard, fast and NO_2 rich, was 8 % O_2, 5 % H_2O, 1000/500/250 ppm NO resp., 0/500/750 ppm NO_2 resp. and argon as balance. The space velocity used was 45,000 h^{-1} (GHSV).

	Fresh		SO_2 exposed		Reg 500 °C		Reg 700 °C	
Temperature	220 °C	280 °C	220 °C	280 °C	220 °C	280 °C	220 °C	280 °C
Standard	94.5	96	25	70.3	91.7	95.6	95.1	97.5
NO_2-rich	99.7	97.9	73.5	96.6	99.7	98.0	99.4	97.8
Fast	99.4	97.7	92.7	96.5	99.1	98.8	99.0	98.0

Apparent rate constant

The activity for NO_x reduction for the samples treated under different conditions was compared using the apparent rate constant. The apparent rate constant is calculated according to equation 4.3 using the assumptions mentioned after the equation. By relating the rate constant for the SO_2-exposed samples to that of the fresh sample, the relative rate constant is obtained.

$$-k = \frac{F_{NO_x,in}}{c_{NO_x,in} \cdot v} ln(1 - \frac{X}{100}) \tag{4.3}$$

Where k is the apparent rate constant [s^{-1}], X is the NO conversion [%], $F_{NOx,in}$ is the molar flow rate of NO_x in the feed [mol s^{-1}], $c_{NOx,in}$ is the concentration of NO_x in the feed [mol dm^3] and V is the catalyst volume [dm^3]. The reaction order was assumed to be first order with respect to NO_x and zero order with respect to NH_3 [31, 96, 97]. The dependence on the ammonia concentration is not actually zero but it is weaker than first order. The error is however the same for all samples since the experiments are performed at the same reaction conditions, hence, the error cancels out when comparing the samples.

Catalyst characterization

To achieve understanding about how the deactivation of the catalyst exposed to SO_2 proceeds on the surface, more information about the catalyst is needed. This information is obtained by different characterization techniques where each one gives a piece of the answer.

Elemental analysis

After exposing the catalyst sample to SO_2, it is of interest to quantify the amount of the sulfur that has adsorbed on the catalyst and possibly relate the amount of sulfur to the degree of deactivation. The amount of sulfur on the catalyst could be measured by several techniques, the one used for these studies is XRF which is described in section 2.4. Using this technique shows that the Cu-CHA sample exposed to SO_2 at the lowest temperature (220 °C) has captured a significantly higher amount of the sulfur when compared to the samples exposed to SO_2 at higher temperatures. This higher uptake of sulfur most likely explains the more severe deactivation observed for this sample in Figure 4.10. For the samples used in the investigation of the impact of SO_2 exposure temperature, an almost linear relationship was found between the sulfur uptake and the relative rate constant.

Surface morphology

It is not only important to know how much sulfur that is adsorbed on the catalyst, the type and availability of metal sites in the catalyst are also important parameters. To study metal particles, STEM is a useful technique for determining particle size and in the case of Cu-CHA, the presence of CuO_x as seen in Figure 4.12. The technique is described in section 2.4 and in **Paper V**.

Temperature-programmed desorption

Adsorbing a compound on a catalyst sample and then desorbing it under a temperature ramp can provide information of the number and type of adsorption sites on the catalyst. One of the most common compounds used to characterize SCR catalysts is ammonia. By using NH_3-TPD it is possible to quantify the number of acidic sites of the catalyst before and after ageing with SO_2 or other catalyst poisons [98–102].

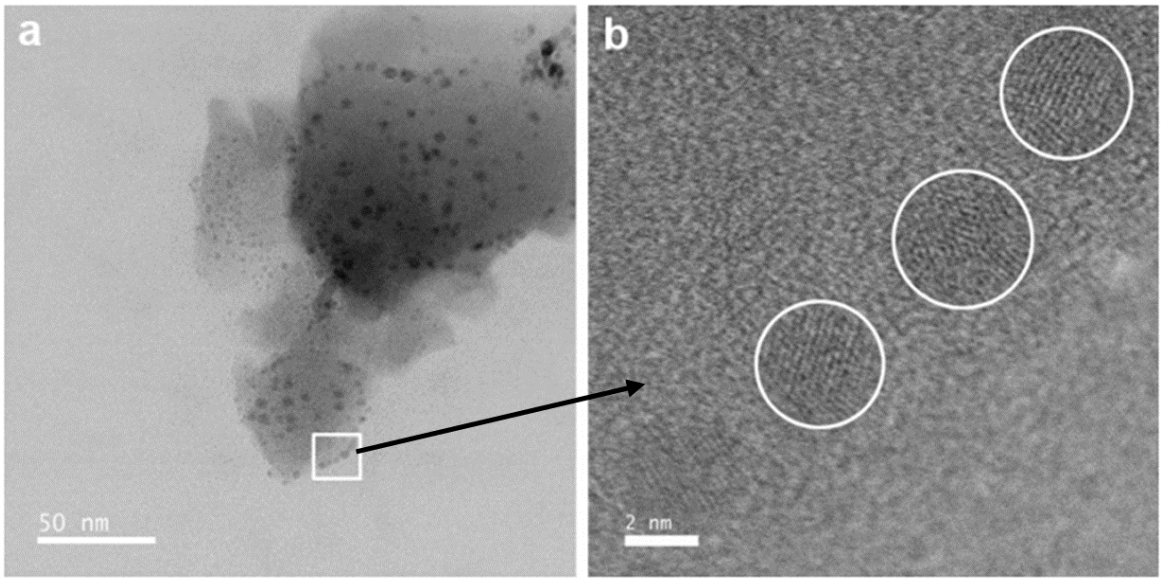

Figure 4.12: STEM images of the fresh Cu-CHA catalyst used for deactivation studies using SO_2. The scales of image a) and b) can be seen in the lower left corner of each image.

Using ammonia-TPD it was found that the amount of adsorbed NH_3 did not change after exposure to SO_2 at temperatures below 300 °C when compared to a fresh sample. However, after SO_2 exposure at higher temperatures, the amount of adsorbed NH_3 increased after SO_2 exposure. This indicates that the sulfur species on the catalyst depend on the exposure temperature and their nature is different in terms of acidity. In order to follow how metallic sites of the Cu-CHA catalyst change after SO_2 exposure, TPD with NO_2 as probe molecule was used. Here the catalyst was exposed to NO_2 at 100 °C in Ar and NO_2, flushed with argon and the finally the temperature was increased to 500 °C at a rate of 10 °C/min whereby the desorbed NO_2 was analyzed. As can be seen in Figure 4.13 there are four peaks originally, representing four types of metallic sites [103]. However, after SO_2 exposure at 220 °C for 8 hours, the peaks are shifted towards lower desorption temperatures and the peak at the highest temperature is absent. After regeneration in O_2 and H_2O with argon as balance, at 500 °C, most of the catalysts ability to adsorb NO_2 is regained and after regeneration at 700 °C, the catalyst can adsorb and desorb over 90 % of the amount it did when fresh. From these results it seems that there is one type of copper site in particular that becomes poisoned by SO_2. Furthermore, the existence of four types of copper sites in the Cu-CHA was confirmed by temperature-programmed reduction using hydrogen, H_2-TPR, in **Paper V**.

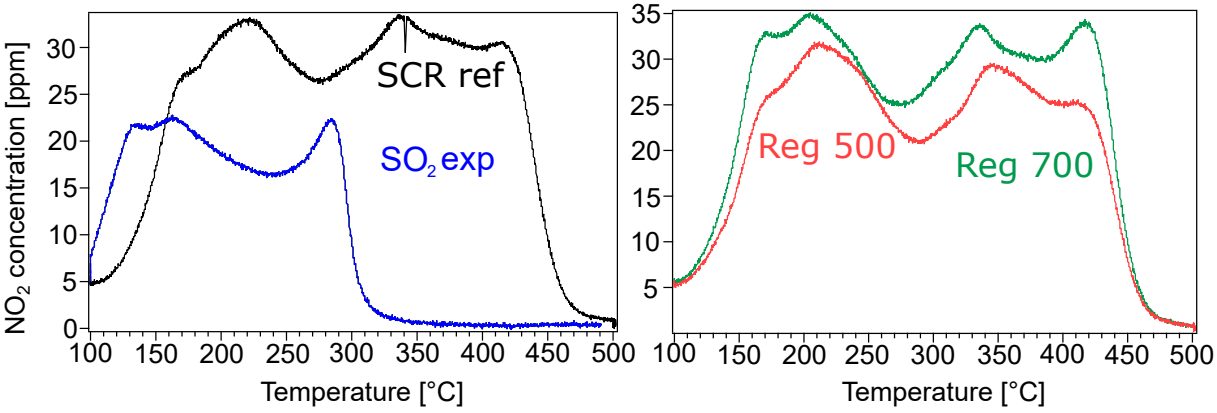

Figure 4.13: NO_2 desorption for a fresh and SO_2-exposed Cu-CHA SCR catalyst (left figure). NO_2 desorption after regeneration at 500 and 700 °C is also presented (right figure). The space velocity used was 45,000 h^{-1} (GHSV).

Cu-sites before and after exposure to SO_2

Using in-situ X-ray absorbtion spectroscopy (XAS) and analyzing the XANES (X-ray absorption near edge structure) and EXAFS (extended X-ray absorption fine structure) the obtained spectra can give information about the nature of the Cu-species in the catalyst before and after exposure to SO_2. In **Paper V**, the Cu-CHA was exposed to high-energy X-ray radiation around the Cu K-edge. Some of the X-rays are absorbed which cause excitation of core electrons. The absorbtion is quantified and then the energy of the X-rays is changed and the procedure is repeated until a desired energy interval is scanned. The reason for using a synchrotron light source is the improved quality and speed of the data collection [104]. The XANES part of the obtained XAS spectra is the lower energy part of the spectra around the absorption edge and from this part of the spectra information about oxidation state and coordination environment could be obtained. The EXAFS part is the higher energy part of the spectra which gives information about coordination number and bond distance in the sample [105]. By using this technique it was found that sulfur primarily adsorbs to the catalyst on isolated Cu species as Cu-bisulfate and some SO_2 also adsorbs on CuO_x clusters found in the Cu-CHA catalyst. The peak that disappears in the NO_2-TPD profile after SO_2 exposure, shown in Figure 4.13, likely corresponds to a single site Cu species.

4.3.1 Summary of the ageing results for the single poison ageing of the SCR-catalysts

The degree of impact on the Cu-CHA SCR catalyst from exposure to SO_2 depends on several parameters. One being the temperature at which the SO_2 exposure has been performed. Another relevant aspect is the presence of NO_2 in the exhaust feed when evaluating the SCR performance of the catalyst.

For the temperature during SO_2 exposure it was concluded that the lowest exposure temperature, within the range tested (220-400 °C), results in a more severe deactivation when compared to the other temperatures tested. The higher the exposure temperature, the lower impact it has on the NO_x reduction performance under standard SCR conditions. The same was found for fast SCR conditions, however the presence of NO_2 in the feed contributes to an overall higher conversion of NO_x and a lower degree of deactivation after SO_2 exposure. It was also found that after regeneration of the catalyst at 500 °C, most of the activity towards NO_x reduction was regained and after a subsequent regeneration at 700 °C the activity of the catalyst catalyst was close to that of the fresh catalyst. Furthermore,it was shown that the Cu-CHA catalyst most likely contains four types of metallic sites and the sulfur, in the form of SO_2, primarily forms Cu-bisulfate species on isolated copper sites.

4.4 Summary of the ageing results for the SCR-catalyst

The SCR catalyst in a typical Euro VI heavy-duty vehicle has several up-stream components that function as buffers against poisoning of the catalyst. The up-stream oxidation catalyst as well as the particulate filter will capture catalyst poisons like sulfur and phosphorus which helps the SCR catalyst to remain active for a longer time.

When performing engine-bench ageing as well as diesel burner ageing, the presence of up-stream components of the emission control system shield the SCR catalyst, which becomes less deactivated after exposure to biogas and biodiesel exhaust when compared to an SCR catalyst without up-stream components. One of the most potent catalyst poisons for both the vanadium based SCR catalyst and the copper-exchanged CHA SCR catalyst is phosphorus. However, phosphorus appears to adsorb on the first surface it comes in contact with, which means that an up-stream component will hinder most of the phosphorus to reach the down-stream SCR catalyst. When the concentration of phosphorus is high in the exhaust feed, like it was for the diesel burner experiments, the phosphorus is found throughout the catalyst and not only on the inlet part. Phosphorus adsorbs non-selectively on the SCR catalyst while sulfur adsorbs more selectively on the metallic sites of the Cu-CHA catalyst. Sulfur only sticks to the vanadium based catalyst in low amounts.

The deactivation of the SCR catalyst is not only dependent on the catalyst poisons, the temperature at which the exposure to poison occurs is also of major importance. It was shown in **Paper III** that SO_2 exposure at a low temperature (220 °C) results in a considerably more severe deactivation of the Cu-CHA catalyst compared to exposure at higher temperatures. The degree of deactivation caused by exposure to SO_2 is also dependent on the presence of NO_2 in the feed during NO_x reduction. Under fast SCR conditions, when 50 % of the inlet NO_x is NO_2, the impact from SO_2 exposure is not as severe as if no NO_2 is present in the feed (standard SCR conditions). During SO_2 exposure at low temperatures it appears that the SO_2 mainly interacts with isolated copper species forming Cu-bisulfates.

Exposure to biofuels, which contain catalyst poisons, causes deactivation of all parts in the emission control system including the SCR catalyst, independently of which type SCR catalyst that is used. The degree of deactivation depends on the type of catalyst and catalyst poison, poison exposure temperature and NO_2 concentration in the exhaust feed. Likely it also depends on several other parameters but these aspects are covered in the present work and they all play an important role for the lifetime of the SCR catalyst.

CHAPTER 5
SYSTEM OUTLOOK

When studying deactivation of an emission control system it is important to not only study the individual parts without taking into consideration the entire system. The novelty of the project presented in this thesis is that the entire emission control system is studied and the impact on the entire system is also taken into consideration when discussing deactivation of each part. Naturally, only components down-stream are impacted from changes to each part of the emission control system since the exhaust gas only flows one way, hence the main focus has been the impact on the SCR catalyst following deactivation of the oxidation catalyst and the particulate filter. This final part of the thesis considers all the results and conclusions presented in this thesis with a system approach.

5.1 Synergy effects

When the combined effect of two events sum up to more than the combination of the two individual events we talk about synergy effects. When putting it into the context of emission control systems it could mean that the deactivation of two different parts in the system sum up to a more severe deactivation than just the linear combination of the two. In the full Euro VI system studied in this thesis it could be that the deactivation of the oxidation catalyst has an impact on the SCR catalyst. This has been shown and discussed throughout the thesis and it has been shown that the NO_2 concentration in the exhaust feed is of major importance for the efficiency of the SCR catalyst especially

after deactivation by sulfur poisoning. The majority of the NO_x comes out from the engine in the form of NO which means that the oxidation catalyst and the particulate filter, which have noble metal coatings, are essential for obtaining fast SCR conditions. This is due to the fact that these two components oxidize NO into NO_2 and if the oxidation catalyst becomes deactivated it is shown in this thesis that the conversion of NO into NO_2 decreases at temperatures below 300 °C. This means that not only do the SCR catalyst become deactivated over time and loses activity. At low temperatures the reaction condition is over time more likely to be standard SCR condition, due to the decreased formation of NO_2 in the oxidation catalyst, which is not as effective for removing NO_x from the exhaust. The deactivation of the oxidation catalyst leads to a decrease in efficiency of the SCR catalyst at the same time as the SCR catalyst itself becomes less effective at reducing NO_x over time. It has been shown that the exposure to SO_2 is detrimental to the Cu-CHA catalyst and in particular under standard SCR conditions, the NO_x reduction decreases significantly which means that if the NO_2/NO_x ratio can be kept around 0.5, the impact of the deactivation is not as severe. Unfortunately at lower temperatures, it has been shown that keeping the NO_2 formation optimal is difficult. One suggestion to prevent rapid and severe deactivation of the first component in the emission control system may be to install a poison trap, which captures catalyst poisons up-stream of the oxidation catalyst. The requirements for this device would, however be demanding since no or only marginal pressure drop should occur over it and it is also important that it does not create a decrease in exhaust temperature for the down-stream components to perform efficiently.

Acknowledgements

The research presented in this thesis was carried out at the Division of Applied Chemistry and the Competence Centre for Catalysis (KCK), Chalmers University of Technology, Göteborg, Sweden, during the period July 2014 to May 2020.

The work is financially supported by the Swedish Energy Agency through the FFI program "Interplay effects in deactivation of aftertreatment catalysts for bio fueled engines" (No. 38364-1) and the Competence Centre for Catalysis, which is hosted by Chalmers University of Technology and financially supported by the Swedish Energy Agency and the member companies AB Volvo, ECAPS AB, Johnson Matthey AB, Preem AB, Scania CV AB, Umicore Denmark ApS and Volvo Car Corporation AB.

I would also like to thank:

My supervisor Magnus Skoglundh for supporting and caring for me. For our scientific discussions and our non-scientific discussions. My co-supervisor Per-Anders Carlson for all nice input and discussions, I have enjoyed working with you both.

The 3SAM group and our hangarounds:) Our group has been great both in terms of science discussions and social events. I will miss our meetings and dinners.

The "Johanna at KTH" aka Sandra Dahlin. Without whom this project would have been much less rewarding and educational. I must say that you are the best thing that came out of this project for me since I in you see a life-time friend. I will for sure miss going to conferences with you and I do think conferences will miss us! You and your family are always welcome to the front side of Sweden for a visit.

LoL aka Lasse Urholm and Lennart Norberg who have made the time in the lab so much more easy and talking to you always make me happy. I will miss you both so much.

Anne Wendel for beeing a great friend and colleague. For all your support and help and the fikas and lunches. Meeting you in the fika room each morning before anyone else got there always brightened my day.

Hanna Härelind for being my examiner and supporter in both my research and personal life. You have helped me through this and I'm eternally grateful.

Carina, Frida and Ann who have helped me with all things not related to science and you all have helped lifting the spirit at work with your amazing personalities.

Since I have been at Chalmers for so long now there have been many colleagues passing by and I can't mention all of you here but all of you have contributed to my well-being during this time. I'm happy to say that some of you have become great friends of mine.

The best roomie anyone could ask for, CR, you have been a rock and I know that we will continue our friendship after this journey. I will forever be happy that you got the position and the empty spot in my office.

My very supporting friends Maya, Maddie and Saba, you are so amazing women and I really look up to all of you and I'm so crazy happy to have you and your families in my life. My sisters by choice.

My parents and siblings for always being there for me, I love you all. Mamma och pappap tack för att ni alltid hjälpt mig med allt och funnits där som stöd. Jossan och Niklas, vad vore jag utan er?? Ni har format mig till den jag är och jag vet att ni alltid kommer finnas där för mig. This extends to my husbands family as well, you are all important to me!

My core, my life, the loves of my life, Sigrid and Rut you came to me during this time in my life and I love you so much it hurts. You are the best thing that have happened to me and even though it is challenging I would never go back. SIGRID OCH RUT, JAG ÄLSKAR ER! My husband for being there and helping me raising our daughters and supporting me in all I do. The three of you are my pack and we will always belong together.

Johanna Englund, Göteborg, April 2020

BIBLIOGRAPHY

[1] J. J. Berzelius, *Jahres-Bericht*, 1835, **14**, 234.

[2] M. Rayner-Canham and G. Rayner-Canham, *Women in Chemistry: Their Changing Roles from Alchemical Times to the Mid-twentieth Century*, History of modern chemical sciences, Chemical Heritage Foundation, 1998.

[3] J. G. de Vries and S. D. Jackson, *Catal. Sci. Technol.*, 2012, **2**, 2009–2009.

[4] H. Steinhagen and G. Helmchen, *Angewandte Chemie International Edition in English*, 1996, **35**(20), 2339–2342.

[5] A. Bruggink, R. Schoevaart, and T. Kieboom, *Organic Process Research & Development*, 2003, **7**(5), 622–640.

[6] J. G. J. Olivier, J. A. V. Aardenne, F. J. Dentener, V. Pagliari, L. N. Ganzeveld, and J. A. H. W. Peters, *Environmental Sciences*, 2005, **2**(2-3), 81–99.

[7] Dieselnet emission standards `https://dieselnet.com/standards/` accesed 2020-03-13, 2020.

[8] Timeline of major accomplishments in transportation, air pollution, and climate changes `https://www.epa.gov/transportation-air-pollution-and-climate-change/timeline-major-accomplishments-transportation-air` accesed 2020-03-13, 2020.

[9] Regulation (EU) 2019/631, Official journal of the european union, 2019.

[10] Regualtions No 595/2009, Official journal of the european union, 2009.

[11] G. Smedler, O. Sonntag, P. Marsh, and M. Decker, *Potential of the SCRF® concept for future legislation*, In: Liebl J., Beidl C. (eds) Internationaler Motorenkongress

2016, Springer Vieweg, Wiesbaden, Wiesbaden, 2016.

[12] Katalysatorer på äldre bilar https://www.riksdagen.se/sv/dokument-lagar/dokument/motion/katalysatorer-pa-aldre-bilar_GM02MJ793accessed2020-03-13, 2020.

[13] T. Bligaard and J. Nørskov in *Chemical Bonding at Surfaces and Interfaces*, ed. A. Nilsson, L. G. Pettersson, and J. K. Nørskov; Elsevier, Amsterdam, 2008; pp. 255 – 321.

[14] I. Chorkenforff and H. Niemantsverdriet, *Concepts of Modern Catalysis and Kinetics*, John Wiley and Sons, Ltd, 2005.

[15] S. Rood, S. Eslava, A. Manigrasso, and C. Bannister, *Proceedings of the Institution of Mechanical Engineers, Part D: Journal of Automobile Engineering*, 2020, **234**(4), 936–949.

[16] Y. Xinmei, L. Hongqi, and G. Ying, *Emission Control Science and Technology*, 2015, **1**, 121–133.

[17] T. W. Beutel, J. C. Dettling, D. O. Hollobaugh, and T. W. Mueller, Pt-pd diesel oxidation catalyst with co/hc light-off and hc storage function, US patent 7,576,031 B2 Aug. 18, 2009.

[18] E. J. Bissett, *Chemical Engineering Science*, 1984, **39**(7), 1233 – 1244.

[19] M. Koebel, M. Elsener, and M. Kleemann, *Catalysis Today*, 2000, **59**(3), 335 – 345.

[20] M. Koebel and E. O. Strutz, *Industrial & Engineering Chemistry Research*, 2003, **42**(10), 2093–2100.

[21] G. Lapisardi, L. Urfels, P. Gélin, M. Primet, A. Kaddouri, E. Garbowski, S. Toppi, and E. Tena, *Catalysis Today*, 2006, **117**(4), 564 – 568.

[22] A. Ersson, H. Kušar, R. Carroni, T. Griffin, and S. Järås, *Catalysis Today*, 2003, **83**(1), 265 – 277.

[23] N. M. Kinnunen, J. T. Hirvi, M. Suvanto, and T. A. Pakkanen, *Journal of Molecular Catalysis A: Chemical*, 2012, **356**, 20 – 28.

[24] A. Morlang, U. Neuhausen, K. Klementiev, F.-W. Schütze, G. Miehe, H. Fuess, and E. Lox, *Applied Catalysis B: Environmental*, 2005, **60**(3), 191 – 199.

[25] A. T. Gremminger, H. W. P. de Carvalho, R. Popescu, J.-D. Grunwaldt, and O. Deutschmann, *Catalysis Today*, 2015, **258**, 470 – 480.

[26] N. M. Martin, J. Nilsson, M. Skoglundh, E. C. Adams, X. Wang, G. Smedler, A. Raj, D. Thompsett, G. Agostini, S. Carlson, K. Norén, and P.-A. Carlsson, *Catalysis, Structure & Reactivity*, 2017, **3**(1-2), 24–32.

[27] Y. Deng, X. Wang, G. Chen, H. Wu, Z. Han, and R. Li, *ACS Omega*, 2019, **4**(17), 17098–17108.

[28] F. Millo, M. Rafigh, M. Andreata, T. Vlachos, P. Arya, and P. Miceli, *Fuel*, 2017, **198**, 58 – 67.

[29] D. Wang, Y. Jangjou, Y. Liu, M. K. Sharma, J. Luo, J. Li, K. Kamasamudram, and W. S. Epling, *Applied Catalysis B: Environmental*, 2015, **165**, 438 – 445.

[30] F. Gao, J. H. Kwak, J. Szanyi, and C. H. Peden, *Topics in Catalysis*, 2013, **56**, 1441–1259.

[31] J. H. Kwak, D. Tran, J. Szanyi, C. H. F. Peden, and J. H. Lee, *Catalysis Letters*, 2012, **142**, 295–301.

[32] J. Granestrand, S. Dahlin, O. Immele, L. Schmalhorst, C. Lantto, M. Nilsson, R. S. París, F. Regali, and L. J. Pettersson, *RSC Catalysis*, 2018, **30**, 64–145.

[33] S. J. Schmieg, S. H. Oh, C. H. Kim, D. B. Brown, J. H. Lee, C. H. Peden, and D. H. Kim, *Catalysis Today*, 2012, **184**(1), 252 – 261.

[34] X. Hou, S. J. Schmieg, W. Li, and W. S. Epling, *Catalysis Today*, 2012, **197**(1), 9 – 17.

[35] K. Leistner, O. Mihai, K. Wijayanti, A. Kumar, K. Kamasamudram, N. W. Currier, A. Yezerets, and L. Olsson, *Catalysis Today*, 2015, **258**, 49 – 55.

[36] H. Kamata, K. Takahashi, and I. Odenbrand, *Catalysis Letters*, 1998, **53**(1-2), 65–71.

[37] S. Dahlin, M. Nilsson, D. Bäckström, S. L. Bergman, E. Bengtsson, S. L. Bernasek, and L. J. Pettersson, *Applied Catalysis B: Environmental*, 2016, **183**, 377–385.

[38] D. Nicosia, I. Czekaj, and O. Kröcher, *Applied Catalysis B: Environmental*, 2008, **77**(3), 228–236.

[39] L. Chen, J. Li, and M. Ge, *Chemical Engineering Journal*, 2011, **170**(2), 531–537.

[40] M. Klimczak, P. Kern, T. Heinzelmann, M. Lucas, and P. Claus, *Applied Catalysis B: Environmental*, 2010, **95**(1), 39–47.

[41] O. Kröcher and M. Elsener, *Applied Catalysis B: Environmental*, 2008, **77**(3), 215–227.

[42] R. Khodayari and C. Odenbrand, *Applied Catalysis B: Environmental*, 2001, **30**(1), 87 – 99.

[43] A. Molino, F. Nanna, Y. Ding, B. Bikson, and G. Braccio, *Fuel*, 2013, **103**, 1003 – 1009.

[44] T. Patterson, S. Esteves, R. Dinsdale, A. Guwy, and J. Maddy, *Bioresource Technology*, 2013, **131**, 235 – 245.

[45] T. Korakianitis, A. Namasivayam, and R. Crookes, *Progress in Energy and Combustion Science*, 2011, **37**(1), 89 – 112.

[46] E. Sendzikiene, V. Makareviciene, and P. Janulis, *Renewable Energy*, 2006, **31**(15), 2505 – 2512.

[47] J. Herreros, S. Gill, I. Lefort, A. Tsolakis, P. Millington, and E. Moss, *Applied Catalysis B: Environmental*, 2014, **147**, 835 – 841.

[48] M. H. Wiebenga, C. H. Kim, S. J. Schmieg, S. H. Oh, D. B. Brown, D. H. Kim, J.-H. Lee, and C. H. Peden, *Catalysis Today*, 2012, **184**(1), 197 – 204.

[49] B. M. Shakya, B. Sukumar, Y. M. L.-D. Jesús, and P. Markatou, *SAE International Journal of Engines*, 2015, **8**(3), 1271–1282.

[50] X. Auvray and L. Olsson, *Applied Catalysis B: Environmental*, 2015, **168-169**, 342 – 352.

[51] M. Haneda, K. Suzuki, M. Sasaki, H. Hamada, and M. Ozawa, *Applied Catalysis A: General*, 2014, **475**, 109 – 115.

[52] P. Velin, M. Ek, M. Skoglundh, A. Schaefer, A. Raj, D. Thompsett, G. Smedler, and P.-A. Carlsson, *The Journal of Physical Chemistry C*, 2019, **123**(42), 25724–25737.

[53] C.-R. Florén, M. Van den Bossche, D. Creaser, H. Grönbeck, P.-A. Carlsson, H. Korpi, and M. Skoglundh, *Catal. Sci. Technol.*, 2018, **8**, 508–520.

[54] H. Kannisto, H. H. Ingelsten, and M. Skoglundh, *Journal of Molecular Catalysis A: Chemical*, 2009, **302**(1), 86 – 96.

[55] N. Sadokhina, G. Smedler, U. Nylén, M. Olofsson, and L. Olsson, *Applied Catalysis B: Environmental*, 2017, **200**, 351 – 360.

[56] S. Mulla, N. Chen, L. Cumaranatunge, G. Blau, D. Zemlyanov, W. Delgass, W. Epling, and F. Ribeiro, *Journal of Catalysis*, 2006, **241**(2), 389 – 399.

[57] Stefan Hüfner, *Photoelectron Spectroscopy Principles and Applications*, Springer-Verlag Berlin Heidelberg GmbH, 3rd ed., 2003.

[58] S. Hüfner and T. Huber, *Photoelectron Spectroscopy: Principles and Applications*, Advanced Texts in Physics, Springer, 2003.

[59] J. Oi-Uchisawa, S. Wang, T. Nanba, A. Ohi, and A. Obuchi, *Applied Catalysis B: Environmental*, 2003, **44**(3), 207 – 215.

[60] D. Fino, S. Bensaid, M. Piumetti, and N. Russo, *Applied Catalysis A: General*, 2016, **509**, 75 – 96.

[61] D. S. Su, A. Serafino, J.-O. Müller, R. E. Jentoft, R. Schlögl, and S. Fiorito, *Environmental Science & Technology*, 2008, **42**(5), 1761–1765.

[62] Y. Deng, X. Wang, G. Chen, H. Wu, Z. Han, and R. Li, *ACS Omega*, 2019, **4**(17), 17098–17108.

[63] J. Rodríguez-Fernández, M. Lapuerta, and J. Sánchez-Valdepeñas, *Renewable Energy*, 2017, **104**, 30 – 39.

[64] Z. Li, J. Li, S. Liu, X. Ren, J. Ma, W. Su, and Y. Peng, *Catalysis Today*, 2015, **258**, 11 – 16.

[65] L. Chen, J. Li, and M. Ge, *Environmental Science and Technology*, 2010, **44**(24), 9590–9596.

[66] F. Gao, Y. Wang, N. M. Washton, M. Kollár, J. Szanyi, and C. H. F. Peden, *ACS Catalysis*, 2015, **5**(11), 6780–6791.

[67] L. Ma, Y. Cheng, G. Cavataio, R. W. McCabe, L. Fu, and J. Li, *Chemical Engineering Journal*, 2013, **225**, 323 – 330.

[68] J. Song, Y. Wang, E. D. Walter, N. M. Washton, D. Mei, L. Kovarik, M. H. Engelhard, S. Prodinger, Y. Wang, C. H. F. Peden, and F. Gao, *ACS Catalysis*, 2017, **7**(12), 8214–8227.

[69] K. Wijayanti, K. Xie, A. Kumar, K. Kamasamudram, and L. Olsson, *Applied Catalysis B: Environmental*, 2017, **219**, 142 – 154.

[70] Y. Jangjou, Q. Do, Y. Gu, L.-G. Lim, H. Sun, D. Wang, A. Kumar, J. Li, L. C. Grabow, and W. S. Epling, *ACS Catalysis*, 2018, **8**(2), 1325–1337.

[71] Y. Shan, X. Shi, Z. Yan, J. Liu, Y. Yu, and H. He, *Catalysis Today*, 2019, **320**, 84 – 90.

[72] M. Iwasaki and H. Shinjoh, *Applied Catalysis A: General*, 2010, **390**(1), 71 – 77.

[73] M. Colombo, I. Nova, and E. Tronconi, *Catalysis Today*, 2010, **151**(3-4), 223–230.

[74] A. Grossale, I. Nova, and E. Tronconi, *Catalysis Today*, 2008, **136**(1-2), 18–27.

[75] M. Koebel, G. Madia, and M. Elsener, *Catalysis Today*, 2002, **73**(3-4), 239–247.

[76] E. Tronconi, I. Nova, C. Ciardelli, D. Chatterjee, and M. Weibel, *Journal of Catalysis*, 2007, **245**(1), 1 – 10.

[77] C. Paolucci, I. Khurana, A. A. Parekh, S. Li, A. J. Shih, H. Li, J. R. Di Iorio, J. D. Albarracin-Caballero, A. Yezerets, J. T. Miller, W. N. Delgass, F. H. Ribeiro, W. F. Schneider, and R. Gounder, *Science*, 2017, **357**(6354), 898–903.

[78] G. He, Z. Lian, Y. Yu, Y. Yang, K. Liu, X. Shi, Z. Yan, W. Shan, and H. He, 11 , 2018, **4**, eaau4637.

[79] T. V. W. Janssens, H. Falsig, L. F. Lundegaard, P. N. R. Vennestrøm, S. B. Rasmussen, P. G. Moses, F. Giordanino, E. Borfecchia, K. A. Lomachenko, C. Lamberti, S. Bordiga, A. Godiksen, S. Mossin, and P. Beato, *ACS Catalysis*, 2015, **5**(5), 2832–2845.

[80] M. Koebel, G. Madia, and M. Elsener, 04 , 2002, **73**, 239–247.

[81] M. Hochella and A. Carim, *Surface Science*, 1988, **197**(3), L260 – L268.

[82] S. Dahlin, *Deactivation of emission control catalysts for heavy-duty vehicles – Impact of biofuel and lube oil-derived contaminants*, Kungliga Tekniska Högskolan, Stockholm, 2020.

[83] M. Magnusson, E. Fridell, and H. H. Ingelsten, *Applied Catalysis B: Environmental*, 2012, **111-112**, 20 – 26.

[84] W. S. Kijlstra, N. J. Komen, A. Andreini, E. K. Poels, and A. Bliek in *11th International Congress On Catalysis - 40th Anniversary*, ed. J. W. Hightower, W. N. Delgass], E. Iglesia, and A. T. Bell, Vol. 101 of *Studies in Surface Science and Catalysis;* Elsevier, 1996; pp. 951 – 960.

[85] J. Kagawa, *Toxicology*, 2002, **181-182**, 349 – 353.

[86] P. S. Hammershøi, A. D. Jensen, and T. V. Janssens, *Applied Catalysis B: Environmental*, 2018, **238**, 104 – 110.

[87] P. S. Hammershøi, Y. Jangjou, W. S. Epling, A. D. Jensen, and T. V. Janssens, *Applied Catalysis B: Environmental*, 2018, **226**, 38 – 45.

[88] R. Ando, T. Hihara, Y. Banno, M. Nagata, T. Ishitsuka, N. Matsubayashi, and T. Tomie In *SAE Technical Paper*. SAE International, 2017.

[89] M. Shen, Z. Wang, X. Li, J. Wang, J. Wang, and C. Wang, 08 , 2019, **36**, 1249–1257.

[90] A. J. Shih, I. Khurana, H. Li, J. González, A. Kumar, C. Paolucci, T. M. Lardinois, C. B. Jones, J. D. A. Caballero], K. Kamasamudram, A. Yezerets, W. N. Delgass, J. T. Miller, A. L. Villa, W. F. Schneider, R. Gounder, and F. H. Ribeiro, *Applied Catalysis A: General*, 2019, **574**, 122 – 131.

[91] Y. Jangjou, C. S. Sampara, Y. Gu, D. Wang, A. Kumar, J. Li, and W. S. Epling, *React. Chem. Eng.*, 2019, **4**, 1038–1049.

[92] J. Li, Y. Peng, H. Chang, X. Li, J. Rittenden, and J. Hao, 03 , 2016, **10**.

[93] S. Cimino and L. Lisi, *Catalysts*, 2019, **9**(8).

[94] J. Luo, H. An, K. Kamasamudram, N. Currier, A. Yezerets, T. Watkins, and L. Allard, *SAE International Journal of Engines*, 2015, **8**(3), 1181–1186.

[95] W. Shan and H. Song, *Catal. Sci. Technol.*, 2015, **5**, 4280–4288.

[96] F. Gao, E. D. Walter, M. Kollar, Y. Wang, J. Szanyi, and C. H. Peden, *Journal of Catalysis*, 2014, **319**, 1 – 14.

[97] S. A. Bates, A. A. Verma, C. Paolucci, A. A. Parekh, T. Anggara, A. Yezerets, W. F. Schneider, J. T. Miller, W. N. Delgass, and F. H. Ribeiro, *Journal of Catalysis*, 2014, **312**, 87 – 97.

[98] J. Luo, K. Kamasamudram, N. Currier, and A. Yezerets, *Chemical Engineering Science*, 2018, **190**, 60 – 67.

[99] F. Gao, N. M. Washton, Y. Wang, M. Kollár, J. Szanyi, and C. H. Peden, *Journal of Catalysis*, 2015, **331**, 25 – 38.

[100] L. Ma, W. Su, Z. Li, J. Li, L. Fu, and J. Hao, *Catalysis Today*, 2015, **245**, 16 – 21.

[101] L. Ren, Y. Zhang, S. Zeng, L. Zhu, Q. Sun, H. Zhang, C. Yang, X. Meng, X. Yang, and F.-S. Xiao, *Chinese Journal of Catalysis*, 2012, **33**(1), 92 – 105.

[102] C. Fan, Z. Chen, L. Pang, S. Ming, X. Zhang, K. B. Albert, P. Liu, H. Chen, and T. Li, *Applied Catalysis A: General*, 2018, **550**, 256 – 265.

[103] L. Ma, Y. Cheng, G. Cavataio, R. W. McCabe, L. Fu, and J. Li, *Applied Catalysis B: Environmental*, 2014, **156-157**, 428 – 437.

[104] A. S. Hoffman, L. M. Debefve, A. Bendjeriou-Sedjerari, S. Ouldchikh, S. R. Bare, J.-M. Basset, and B. C. Gates, *Review of Scientific Instruments*, 2016, **87**(7), 073108.

[105] S. Calvin, *XAFS for Everyone*, Boca Raton: CRC Press, 2013.